收稿日期：2020-04-26
改回日期：2020-06-09

基金项目：中国地质调查局地质调查项目“内蒙古温都尔庙—镶黄旗地区区域地质调查(编号: DD20190038)”资助。

doi: 10.12029/gc2020Z107

论文引用格式：刘洋, 滕飞, 王文龙, 杨泽黎, 王树庆, 胡晓佳, 郭硕, 何鹏. 2020. 内蒙古北柳图庙幅 1∶50 000 地质图数据库 [J].中国地质，47(S1):63−76.

数据集引用格式：刘洋; 滕飞; 王文龙; 杨泽黎. 内蒙古北柳图庙幅 1∶50 000 地质图数据库 (V1).中国地质调查局天津地质调查中心 [创建机构], 2016.全国地质资料馆 [传播机构], 2020-06-30. 10.35080/data.A.2020.P7; http://dcc.cgs.gov.cn/cn//geologicalData/details/doi/10.35080/data.A.2020.P7

内蒙古北柳图庙幅 1∶50 000地质图数据库

刘洋　滕飞*　王文龙　杨泽黎　王树庆　胡晓佳　郭硕　何鹏

(中国地质调查局天津地质调查中心, 天津 300170)

摘要: 内蒙古北柳图庙幅 (K49E011021)1∶50 000 地质图根据《区域地质调查技术要求 (1∶50 000)》(DD 2019–01) 和行业的其他统一标准及要求, 充分利用 1∶200 000 区域地质、1∶50 000 矿产调查工作资料, 采用数字地质调查系统 (DGSS), 结合 Spot、ETM、Aster 等多种遥感影像对构造及岩性边界不断验证和完善, 最终绘制成图, 是内蒙古温都尔庙—白乃庙地区具有重要参考意义的成果图件之一。图件详细填绘了白乃庙岛弧带的物质组成和构造组合特点, 对志留系、二叠系、白垩系等沉积建造类型进行了重新划分, 把区内侵入岩划分为 4 个期次, 并构建了相对完善的构造演化序列。图幅数据库的数据内容包含有 3 个非正式填图单位、10 个正式地层单位、4 期岩浆事件和 2 期构造变形, 以及 176 个样品的岩石全分析数据, 10 个样品的锆石 U–Pb 年龄数据，数据量为 28.9 MB。该图幅细化了北侧温都尔庙构造带向南侧俯冲过程形成的白乃庙岛弧带的构造、岩浆演化过程, 反映了 1∶50 000 区域地质调查最新示范性成果, 对温都尔庙造山带古生代构造演化具有重要的科学研究价值, 对后续该区域的地质调查工作也具有参考和借鉴意义。该图幅为中国地质调查局第一幅开展智能化区域地质调查填图的试点图幅, 首次实现了中国区域地质调查工作的全流程智能化野外调查。

关键词: 内蒙古；北柳图庙幅；1∶50 000；地质图；数据库；兴蒙造山带；地质调查工程

数据服务系统网址: http://dcc.cgs.gov.cn

1　引言

兴蒙造山带记录了古亚洲洋俯冲、西伯利亚和华北板块碰撞拼合等大量重要信息 (Xiao W J et al., 2003; Jian P et al., 2008; Xu B et al., 2015), 其构造演化过程与古亚洲洋的构造运动密切相关 (Windley B F et al., 2007; Han B F et al., 2011; Xu Z et al., 2012; Zhang X H et al., 2012; 王树庆等, 2019; 赵越等, 2010)。俯冲增生造山与地体拼贴过程造就了兴蒙造山带现有格架 (Coleman R G, 1989; Windley B F et al., 1990; Allen M B et al., 1993, 1995; Sengor A M C et al., 1993; Gao J.et al, 1998; Jahn B M et al., 2000; Windley B F et al.,

第一作者简介：刘洋, 男, 1986 年生, 硕士, 工程师, 主要从事构造地质学及区域地质调查工作； E–mail: 125313766@qq.com。
通讯作者简介：滕飞, 男, 1987 年生, 硕士, 工程师, 主要从事区域地质调查工作； E–mail: 267272916@qq.com。

2007; Xiao W J et al., 2004, 2010; Li Y J et al., 2018, 2020; Yuan Y et al., 2018; 赵磊等, 2019; 赵闯等, 2020)。正确认识兴蒙造山带的演化对于恢复中亚造山带地区的构造历史意义重大。近些年围绕华北板块北缘重要地质问题进行了大量科学研究, 获得了丰富的资料 (吴飞等, 2014; 张维等, 2012; Zhang W et al., 2013; Liu M et al., 2016)。目前多数学者认为古亚洲洋在早古生代经历了南北两侧的双向俯冲 (Xu B et al., 2013; Li Y L et al., 2014; Liu Y J et al., 2017), 并形成了相应的 2 条早古生代岛弧俯冲带 (Jian P et al., 2008)。其中南部俯冲带就位于巴特敖包—白乃庙—温都尔庙地区, 其存在较为完整的俯冲记录, 包含温都尔庙俯冲增生杂岩带和白乃庙岛弧岩浆岩带。

内蒙古北柳图庙幅 1∶50 000 地质图幅区位于华北板块北缘以北的南部俯冲带形成的白乃庙岛弧岩浆岩带之上（图 1）。本区最早于 1976 年由内蒙古自治区地质局区域地质测量队开展了 1∶200 000 镶黄旗幅区域地质测量[1], 并对区内的地层格架、岩浆活动、构造演化等方面做了全面、系统的总结。2008 年, 内蒙古地质矿产勘察院完成了内蒙古自治区锡林郭勒盟太古生庙等 4 幅 1∶50 000 地质矿产调查[2]。2012 年, 中化地质矿山总局内蒙古地质勘查院完成了内蒙古乌兰察布市土木尔台地区 4 幅 1∶50 000 区域矿产地质调查[3], 内蒙古自治区地质调查院完成了内蒙古查干哈达庙—别鲁乌图地区矿产远景调查[4]。此外, 近些年围绕温都尔庙造山带古生界演化, 进行了大量科学研究并积累了丰富的资料 (柳长峰等, 2014; 李俊建等, 2015; 钱筱嫣等, 2017)。这些调查研究为北柳图庙幅地质图的编制奠定了扎实基础。

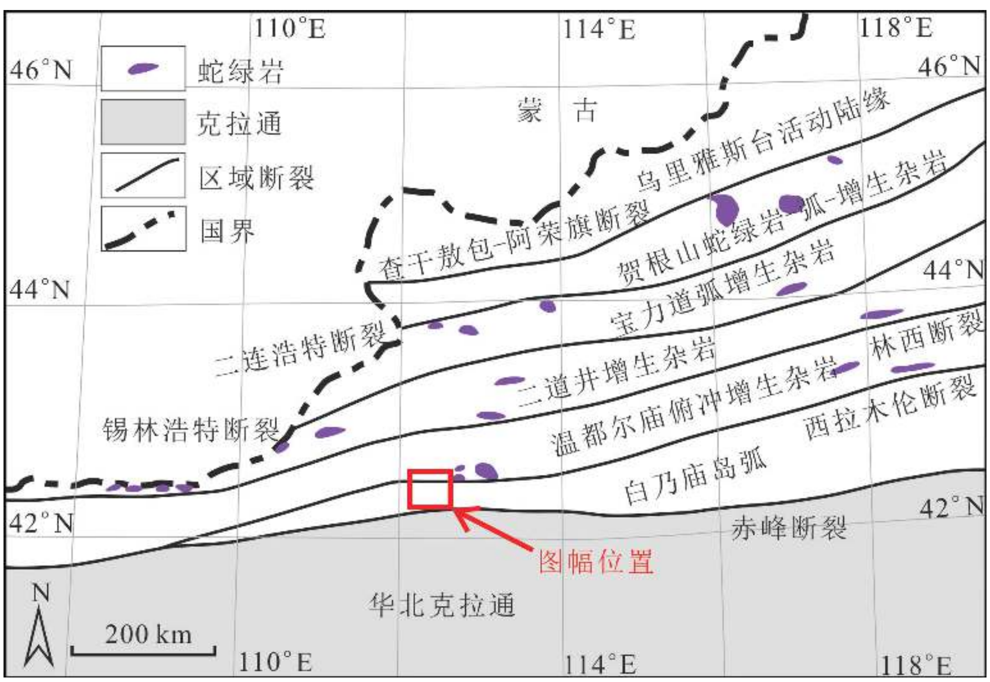

图 1　内蒙古北柳图庙幅 (K49E011021) 大地构造位置图 (据 Xiao WJ et al., 2003 修改)

北柳图庙幅 1∶50 000 地质图作为智能化区域地质调查填图试点的的探索性图件, 力争在客观表达野外地质事实的基础上, 结合前人地质调查、矿产勘查以及科研新成果, 采用最新的填图思路及智能化地质填图方法, 综合造山带构造解析手段 (白瑾, 2003), 精细刻画白乃庙岛弧带的早古生代地质构造演化过程。内蒙古北柳图庙幅 1∶50 000 地质图数据库 (表 1, 刘洋等, 2020) 系统反映了白乃庙古生代地质体的沉积建造、构造组合样式与时代属性, 从而为温都尔庙地区地质科研和野外地质调查提供有益的参考资料。

表 1　数据库 (集) 元数据简介

条目	描述
数据库(集)名称	内蒙北柳图庙幅1：50 000地质图数据库
数据库(集)作者	沉积岩类: 刘　洋, 中国地质调查局天津地质调查中心 火山岩类: 滕　飞, 中国地质调查局天津地质调查中心 岩浆岩类: 王文龙, 中国地质调查局天津地质调查中心 变质岩类: 杨泽黎, 中国地质调查局天津地质调查中心
数据时间范围	2016—2018年
地理区域	经纬度: 东经113°00′ ~ 113°30′; 北纬42°00′ ~ 42°20′
数据格式	MapGIS
数据量	28.9 MB
数据服务系统网址	http://dcc.cgs.gov.cn
基金项目	中国地质调查局地质调查项目“内蒙古温都尔庙-镶黄旗地区区域地质调查” (项目编号: DD20190038)
语种	中文
数据库(集)组成	北柳图庙幅1：50 000地质图数据库包括: 1：50 000地质图库、角图和图饰。地质图库包括沉积岩、火山岩、侵入岩、第四系、构造形迹、地质界线、产状、矿化(点)、蚀变、岩性花纹、各类代号等。角图包括综合柱状图、侵入岩填图单位、图切剖面、大地构造位置图。图饰包括接图表、图例、责任表等

2　数据采集和处理方法

2.1　数据基础

内蒙古北柳图庙幅 1：50 000 地质图以《1：50 000 区域地质调查技术要求》(DD 2019–01) 为规范, 在参考 1：50 000 矿产地质调查项目原始资料 (包括地质草图、遥感解译影像) 的基础上, 根据项目野外实际资料 (实际材料图、剖面图) 重新连图而成, 代表北柳图庙幅 1：50 000 最新地质填图新成果。地理底图采用国家测绘地理信息局最新地理数据。应用已有的技术标准和数字填图系统 (DGSS)、MapGIS 等计算机软件进行数据处理。

2.2　数据处理过程

2.2.1　预研究数据库

预研究数据库主要包括各类遥感影像、卫星影像、物化探图件, 各类图件经核查可用后, 校正配准套在 1：50 000 标准图框及数字地形中, 形成野外工作底图投影系统为高斯–克吕格投影参数, 坐标系统为 2000 国家大地坐标系 (CGCS 2000)。进一步结合 1：200 000 地质图、1：50 000 矿产地质图, 编制地质草图, 所有子图号、岩石代号均按照《1：50 000 区域地质图图例》(GB 958−99) 进行标准化, 在此基础上编制工作部署图, 参考内蒙古岩石地层清理及前人研究成果, 初步划分野外填图单位, 并编制数字填图字典库, 供野外地质调查参考使用。

2.2.2　野外原始数据库

根据已有资料的综合分析和地质草图的编制, 划分重点工作区和一般工作区, 确定了重点填图内容为白乃庙岛弧带火山岩及岩浆岩, 并对复杂区进行了路线加密。原始数据库整体又可分为数字填图资料和数字剖面库。

数字填图资料以 1：25 000 底图为基础, 通过野外实际路线调查, 在数字填图系统中

采集地质点和地质界线及路线等点、线信息, 观察并录入各点的性质、岩性、产状等信息, 形成野外手图。野外手图库存储野外地质路线各类地质数据, 是最重要的野外第一手原始资料数据库。在野外手图库检查无误的基础上, 对所有地质路线内容进行入库汇总整合, 形成野外 PRB 总图库。并将实体观测数据点、线采集层及标注图层进一步继承到实际材料图库中。一般来说, 野外手图整理按照以下步骤进行:

(1) 野外手图的规范处理: 将野外采集的手图资料导入电脑, 补充、完善细化地质点 (P)、点间路线 (R)、界线 (B)、产状、采样、照片对话框与属性框中各项内容, 并保持整体协调一致, 确保客观描述信息无误。

(2) 野外手图的整饰处理: 结合地形、遥感资料, 按“V”字形法则勾绘界线, 对于 U 型路线, 必须确保两侧界线相互对应, 在此基础上, 按照规范要求的线型、子图号及颜色进行处理, 整饰圆滑, 并在点间增加岩性标注信息, 便于后续连图。

(3) 野外手图的综合整理: 结合目标任务, 进行野外路线小结, 系统梳理地层、岩浆岩及构造信息, 对接触关系、构造变形等重要地质现象要专门处理, 整体数据质量检查及自检无误, 提交项目负责入库连图。

数字剖面库采用数字剖面测量方式进行, 以野外工作手图为底图, 在充分踏勘的基础上, 选择出露完整地段进行。野外逐层分层进行, 记录岩性、样品、产状、照片、构造变形等信息, 并在野簿上相应做信手剖面图, 均按系统自动生成的文件名及根据需要自定义文件名进行存储。一般在测量完整剖面后, 由剖面的记录者进行剖面的初步整理和野外小结, 结合室内薄片鉴定, 画剖面图及剖面柱状图。

2.2.3 实际材料图

实际材料图是用点、线、面的空间实体在地形图上表示地质点、地质界线、分段路线、地质体、样品、产状、GPS 点等各种地质要素分布密度的一种重要的原始资料地质图件。1∶50 000 区域地质调查包括实际材料图在内的原始资料原则要求用 1∶25 000 比例尺图幅。一般来说, 野外手图整理按照以下步骤进行:

(1) 地质体界线的形成。实际材料图库中用于连图的线图层文件名为 Geoline.wl, 为建立拓扑关系, 形成地质体面, 其内容除地质体界线外, 还包括内图框线及面状水体、雪山、沙漠等界线, 其中后者从相关图层直接拷贝获取。注: 不分割地质体面的整饰界线不归入 Geoline.wl 图层, 如部分岩相界线、未经证实的遥感解译断层、变质相带等。

(2) 地质体面的形成。地质体界线形成后通过拓扑可形成地质体面实体, 主要通过地质体线转弧段, 进行拓扑重建并进行错误检查, 新生成的临时区文件没有属性结构, 将其合并至实际材料图库地质体区文件中。

(3) 地质体赋属性。数字实际材料图线、面文件形成并赋予属性结构后, 必须对其属性内容进行补充完善。主要包括: 地质体界线属性提取, 地质体面实体属性提取, 根据地质体面自动给界线赋左右地质体代号, 浏览编辑实际材料图属性等步骤。

(4) 实际材料图的整理。主要包括对不同地质体根据属性进行统一着色, 根据相关标准规范对地质体不同类型界线线型及对应参数进行修改, 按规范对地质体代号进行标注, 对图廓外进行整饰, 重点是图例的完善, 将实际材料图库中系统自动生成的无用的空文件删除。

2.2.4 编稿原图

编稿原图等同于地质图, 1∶50 000 编稿原图是在 1∶25 000 实际材料图基础上形成。在形成编稿原图后需要进行全面性、规范性、标准化整理。具体包括: 地质体界线

图层、地质体面图层、产状图层、地质图整饰图层、地质体标注、图外整饰图层、编稿原图库文件等图层及文件的整理流程。在编稿原图库中将系统自动生成的无内容的空文件删除, 在编稿原图工程文件中将野外地质采集图层文件删除, 仅保留与地质图相关的图层文件。

2.2.5 成果空间数据库

空间数据库包括基本要素类、综合要素类、对象类和独立要素类数据库。其中要素数据库是共享空间参考系统的要素类的集合, 在地质图数据模型中, 由地质点、面、线实体类构成。对象类是一个表, 存储非空间数据, 在地质图数据模型中, 一般一个要素类对应多个对象类。地质图基本要素类、综合要素类和对象类各数据项属性齐全。

成果数据库建设内容和有关要求将依据《数字地质图图层及属性文件格式》(D/Z 0197−1997) 等标准进行图形库和属性库等的建设, 参照《地质图用色标准及用色原则》(DZ/T 0179−1997)、《区域地质图图例》(GB 958−99) 等标准确定用色及图饰、图例、符号等的表达。

2.2.6 编制各类角图

内蒙古北柳图庙幅 (K49E011021)1：50 000 地质图主要角图包括: 综合地层柱状图、侵入岩填图单位、图切剖面、大地构造位置图和其他角图 (图 2)。

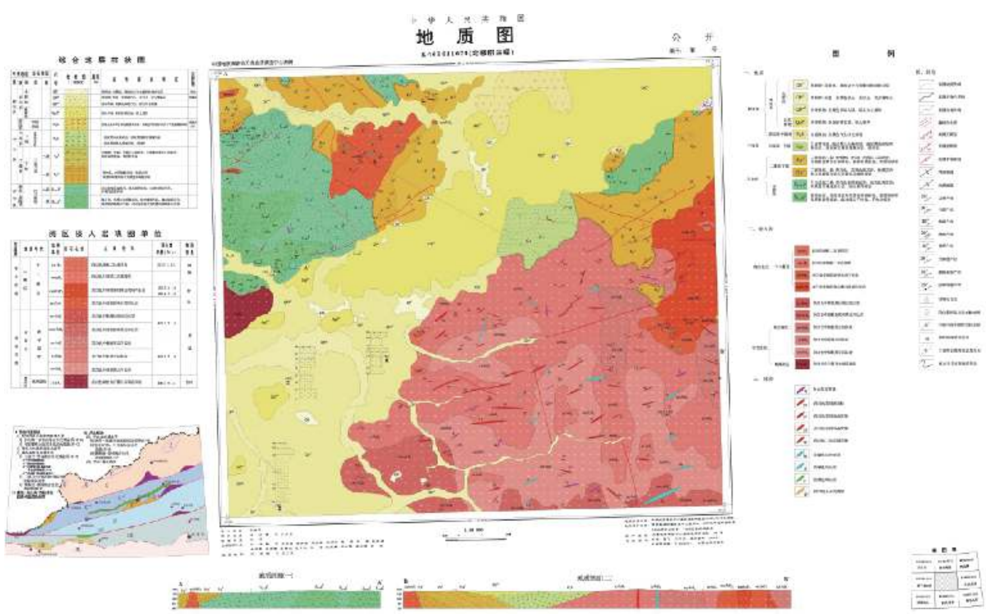

图 2　内蒙古北柳图庙幅 (K49E011021)1：50 000 地质图示意图

(1) 综合地层柱状图: 对不同的岩石地层单元沉积建造特征进行详细表达。系统梳理图幅内各地层单元地层层序、岩石组合特征, 结合锆石测年资料, 综合反映其沉积背景及时代属性。

(2) 侵入岩填图单位: 识别出 4 期岩浆演化序列: ①晚寒武世以发育片麻理的灰白色细粒含石榴白云母花岗岩为代表的俯冲期岩石 (约 500 Ma); ②晚志留世以中粗粒、中粒、中细粒英云闪长岩 (425 Ma) 和中粒、中细粒斑状英云闪长岩 (423 Ma) 为主, 代表了早古生代岛弧构造背景的岩石组合; ③中二叠世早期以中细粒石英闪长岩、中细粒花岗岩闪长岩为主 (约 268 Ma), 代表中二叠世早期挤压构造背景; ④中二叠世晚期以二长花岗岩 (中粒、中细粒) 为主 (约 263 Ma), 代表着构造背景由挤压向伸展构造体制的转换。

(3) 图切剖面: 图幅内建造和构造的总体走向为近北西—北西西向, 为直观表达区内各地质体接触关系及空间位态, 共布置 2 条图切剖面, 对本图幅内各地质体之接触关系进行了较全面控制: ①早古生代岛弧火山岩大比例尺剖面, 结合大比例尺的构造解析, 详细反映了早古生代岛弧带物质组成及构造序列特征; ②北西向纵贯全区剖面, 主要控制整个古生代花岗岩等地质体的空间位态。

(4) 大地构造位置图: 表达了北柳图庙幅在区域大地构造中所处的位置及其大地构造单元划分情况。大地构造位置图体现了温都尔庙洋早古生代向南俯冲形成的沟-弧-盆体系及工作区所处的构造位置。

(5) 其他角图: 对脉岩、地质代号、地质符号及岩性花纹进行梳理, 编制图例及责任表。

3 数据样本描述

3.1 数据的命名方式

地质面.wp, 地质线.wl, 地质点.wt。

3.2 图层内容

主图内容包括沉积岩、火山岩、侵入岩、第四系、构造形迹、地质界线、产状、各类代号等。

角图内容包括地层综合柱状图、侵入岩填图单位、图切剖面、大地构造位置图等。

图饰内容包括接图表、图例、责任表等。

3.3 数据类型

实体类型名称: 点、线、面。

点实体: 各类地质体符号及标记、地质花纹、矿化蚀变。

线实体: 断裂构造、地质界线、岩相界线、构造界线及特殊标志层花纹等。

面实体: 沉积岩、火山岩、变质岩、侵入岩、第四系等。

3.4 数据属性

北柳图庙幅 (K49E011021)1∶50 000 地质图数据库包含地质实体要素信息、地理要素信息和地质图整饰要素信息。地理要素信息属性沿用国家测绘地理信息局提供的数据属性结构。地质实体要素信息属性按照 1∶50 000 区域地质调查专项地质填图数据库建库要求分 4 大岩类 (沉积岩、火山岩、侵入岩、变质岩)、断裂构造、产状要素、矿产地等分别建立数据库属性。

沉积岩建造数据属性主要有: 年代地层单位、岩石地层单位、建造名称、建造代码、岩性组合、地层时代、建造厚度、建造含矿性、岩石结构、沉积构造、岩石颜色、沉积作用类型、沉积相类型、同沉积构造。

火山岩建造数据属性主要有: 年代地层单位、岩石地层单位、建造名称、建造代码、地层时代、地层分区、岩性组合、建造厚度、建造含矿性、火山喷发旋回、火山喷发类型、火山岩成因类型、特殊岩性夹层、火山岩相类型、同位素年龄。

侵入岩建造数据属性主要有: 建造名称、建造代码、岩性组合、建造含矿性、岩石结构、岩石构造、侵入期次、岩体产状、平面形态、剖面形态、岩体侵位构造特征、接触带特征、成因类型、同位素年龄。

变质岩建造数据属性主要有：年代地层单位、岩石地层单位、建造名称、建造代码、岩性组合、地层时代、建造厚度、建造含矿性、岩石结构、岩石构造、原岩建造、变质相、变质作用类型。

断裂构造数据属性主要有：断裂名称、断裂类型、断裂延长、断裂延深、断裂宽度、断裂走向、断裂面倾向、断裂面倾角、断距、断裂面形态、构造岩特征、运动方式、活动期次、力学性质。

产状数据属性有：产状类型、倾向、倾角。

地质图基本要素类、综合要素类和对象类各数据项属性列表见表 2。

表 2　地质图空间数据库数据属性表

数据类型	名称	标准编码	数据项属性
基本要素类	地质体面实体	_GeoPolygon	地质体面实体标识号, 地质体面实体类型代码, 地质体面实体名称, 地质体面实体时代, 地质体面实体下限年龄值, 地质体面实体上限年龄值, 子类型标识
	地质(界)线	_GeoLine	要素标识号, 地质界线代码, 地质界线类型, 界线左侧地质体代号, 界线右侧地质体代号, 界面走向, 界面倾向, 界面倾角, 子类型标识
	产状	_Attitude	要素标识号, 产状类型名称代码, 产状类型名称, 走向, 倾向, 倾角, 子类型标识
	样品	_Sample	要素标识号, 样品编号, 样品类型代码, 样品类型名称, 样品岩石名称, 子类型标识
	照片	_Photograph	要素标识号, 照片编号, 照片题目, 照片说明, 子类型标识
	素描	_Sketch	要素标识号, 素描编号, 素描题目, 素描说明, 子类型标识
	化石	_Fossil	要素标识号, 化石样品编号, 化石所属生物门类, 化石属或种名, 化石产出层位, 含化石地层单位代号, 化石时代, 子类型标识
	同位素测年	_Isotope	要素标识号, 样品编号, 样品名称, 年龄测定方法, 测定年龄, 被测定出地质体单位及代号, 测定分析单位, 测定分析日期, 子类型标识
	火山口	_Crater	要素标识号, 火山口类型, 火山口名称, 火山口大小, 火山口产出的地质体单位及代号, 火山口岩石类型, 火山口形成时代, 子类型标识
	泉	_Spring	要素标识号, 泉类型代码, 泉类型名称, 泉水流量, 泉水温度, 泉的地质体单位及代号, 子类型标识
	河、湖、海、水库岸线	_Line_Geography	要素标识号, 图元类型, 图元名称, 子类型标识
综合要素类	构造变形带	_Tectzone	要素标识号, 变形带代码, 变形带类型名称, 变形带岩石名称, 变形带组构特征, 变形带力学特征, 形成时代, 活动期次, 含矿性, 子类型标
	蚀变带(面)	_Alteration_Polygon	要素标识号, 蚀变类型名称代码, 蚀变类型名称, 蚀变矿物组合及含量, 含矿性, 被蚀变的地质体代号, 子类型标
	火山岩相带	_Volca_Facies	要素标识号, 火山岩岩相类型及代码, 产出的地层单位及代号, 火山岩相岩石类型, 岩石结构, 岩石构造, 流面产状, 流线产状, 形成时代, 含矿性, 子类型标识
	标准图框(内图框)	_Map_Frame	图名, 图幅代号, 比例尺, 坐标系统, 高程系统, 左经度, 下纬度, 图形单位

续表 2

数据类型	名称	标准编码	数据项属性
对象类	沉积(火山)岩岩石地层单位	_Strata	要素分类, 地层单位名称, 地层单位符号, 地层单位时代, 岩石组合名称, 岩石组合主体颜色, 岩层主要沉积构造, 生物化石带或生物组合, 地层厚度, 含矿性, 子类型标识
	侵入岩岩石年代单位	_Intru_Litho_Chrono	要素分类, 岩体填图单位名称, 岩体填图单位符号, 岩石名称(岩性), 岩石颜色, 岩石结构, 岩石构造, 岩相, 主要矿物及含量, 次要矿物及含量, 与围岩接触关系, 围岩时代, 与围岩接触面走向, 与围岩接触面倾向, 与围岩接触面倾角, 流面产状, 流线产状, 形成时代, 含矿性, 子类型标识
	断层	_Fault	要素分类代码, 断层类型, 断层名称, 断层编号, 断层性质, 断层上盘地质体代号, 断层下盘地质体代号, 断层破碎带宽度, 断层走向, 断层倾向, 断层面倾角, 估计断距, 断层形成时代, 活动期次, 子类型标识
	脉岩(面)	_Dike_Object	脉岩分类代码, 脉岩名称, 脉岩符号, 岩性, 颜色, 结构, 构造, 主要矿物及含量, 次要矿物及含量, 与围岩接触面走向, 与围岩接触面倾向, 与围岩接触面倾角, 形成时代, 含矿性, 子类型标识
	非正式地层单位	_INF_STRATA	要素分类代码, 非正式地层单位代码, 岩性, 岩石结构构造, 所含生物化石带或生物组合, 出露宽度或厚度, 含矿性, 所在地层单位符号, 子类型标识
	面状水域	_Water_Region	要素分类代码, 图元类型, 图元名称, 图元特征, 子类型标识
	图幅基本信息	_Sheet_Mapinfo	地形图编号, 图名, 比例尺, 坐标系统, 高程系统, 左经度, 右经度, 上纬度, 下纬度, 成图方法, 调查单位, 图幅验收单位, 评分等级, 完成时间, 出版时间, 资料来源, 数据采集日期

4 数据质量控制和评估

总体按照《区域地质调查技术要求 (1：50 000)》(DD 2019−01) 的填图精度标准进行野外填图。在实际填图过程中, 执行中国地质调查局《区域地质调查技术要求 (1：50 000)》(DD 2019−01) 试行稿中重点突出的要求, 对基岩区采取加密地质路线调查, 对中−新生代地层区采取遥感解译为主、野外验证为辅的方式进行, 在关键区加密布设路线及追索路线, 取得了较好的成果。其中地质点采集以充分控制地质体接触关系、重大构造边界、构造变形、特殊岩性等重要地质界线等为原则。

为填绘北柳图庙幅 1：50 000 地质图, 野外实测入库路线 385 km, 地质点数 993 个, 地质界线数 1 702 个, 薄片鉴定样品 343 件, 岩石全分析样品 176 个, 锆石 U-Pb 年龄样品 10 个, 照片 1 043 张, 实测 1：2 000 地层剖面约 15 km, 实测 1：5 000 侵入岩剖面约 37 km。填图总体精度达到 1：50 000 区域地质专项填图的具体要求。

图面一般只表达直径大于 100 m 的闭合地质体, 宽度大于 50 m、长度大于 250 m 的线状地质体, 以及长度大于 250 m 的断层、褶皱构造。对蛇绿构造混杂岩带中岩块, 则采取适当放大、同类岩块合并的方式予以表达。一般地质点在野外手图上所标定的点位与实地位置误差不得大于 25 m。

数据质量方面，填图路线自检、互检达 100%，项目组抽检 30%，符合地质调查项目质量管理要求。中国地质调查局天津地质调查中心分别于 2016 年 10 月 24 日、2017 年 8 月 10 日、2018 年 10 月 1 日组织有关专家，在野外及室内对项目组原始资料、成果进展进行了质量检查。2018 年 10 月 1 日–6 日，中国地质调查局天津地质调查中心组织专家采用室内、野外现场两者相结合的检查方法对项目进行了野外工作验收，评定为优秀；内蒙古 1∶50 000 北柳图庙等 4 幅区域地质调查子项目最终成果评定为优秀级。

5　数据价值

内蒙古北柳图庙幅 (K49E011021)1∶50 000 地质图是中国地质调查局开展新一轮地质调查工作的代表性图幅之一。该地质图在深入研究本图幅内岩石组合、层序及构造变形的基础上，以最新的造山带填图思路为指导，按照最新《区域地质调查技术要求 (1∶50 000)》(DD 2019−01) 要求，不断完善图面结构与布局，最终以早古生代岛弧结构为核心，通过对沉积建造、岩浆演化序列及构造样式组合特征进行研究，系统建立了北柳图庙地区古生代完整的构造-岩浆-地层演化序列。

5.1　沉积建造特征

对区内地层进行了详细调查研究，查明了各个地层单位的物质组成、地层层序、沉积环境及形成时代，系统地建立了测区岩石地层格架，并进行了非正式岩石地层单位填绘。结合其构造背景，详细划分了沉积建造类型 (表 3)。将白乃庙组重新划分为 2 个段级岩石地层单位，查明了各单位的物质组成、基本层序、沉积环境及变形变质特征。将北柳图庙地区生物碎屑灰岩、含砾砂岩、粉砂岩并具鲍马序列的岩石组合重新厘定为三面井组，并进一步划分为 2 个岩性段。于三面井组一段灰岩中新采得大量䗴类、海百合等化石，为年代地层划分提供了古生物依据，根据化石组合特征及区域对比认为其形成时代为早二叠世。

5.2　构造样式组合特征

对构造格架及变形序列进行详细研究，在区内识别出 2 期褶皱变形：第一期变形发生在早古生代末，为强烈的近南北向的收缩—碰撞构造形成的露头级尺度的纵弯型复式紧闭褶皱；第二期褶皱变形主要发育在晚古生代三面井期之后，并叠加在第一期褶皱作用之上，主要表现为公里级尺度的中常—开阔褶皱，并发育强烈的层片交切关系及劈理折射。

5.3　侵入岩演化序列

对本区侵入岩，以野外岩石组合特征为依据，结合锆石 U-Pb 测年资料，将图幅内侵入岩时代分为晚寒武世、晚志留世、中二叠世早期、中二叠世晚期等 4 期 (表 4)，建立了本区岩浆岩演化序列。

5.4　地球化学测试数据意义

本数据库内包含有图幅区的岩石地球化学测试分析数据 (表 5)，可以反映岩石成因、成岩年龄等重要信息，为内蒙古北柳图庙幅区域地质背景与地质历史演化研究提供科学依据。将原划为奥陶纪的早古生代岛弧侵入岩重新厘定为志留纪，锆石 U-Pb 年龄为 414.4 ~ 434.2 Ma，为俯冲洋壳来源的埃达克岩。该期岩浆事件的识别表明区域早古生代俯冲一直延续到晚志留世 (~ 420 Ma)，对古亚洲洋及兴蒙造山带的演化具有约束意义。

表 3 岩石地层填图单位划分表

年代地层 界	系	统	岩石地层单位划分		地层代号	岩性描述
新生界	第四系	全新统	湖积物		Qh^{l}	由灰黑、灰绿、砂质淤泥、黏土、砂土、砂砾组成
			冲积物		Qh^{al}	位于现代河床中, 由杂色松散堆积的砂砾层、中砂、砂黏土等组成
			洪冲积物		Qh^{pal}	多形成低缓台地, 堆积物主要为黄褐色砂砾、砂及黏土, 砾石分选差, 成分复杂
		上更新统	洪冲积物		Qp_3^{pal}	堆积物主要为黄褐色砂砾、砂及黏土, 分选磨圆差, 成分复杂
	新近系	中新统	汉诺坝组		N_1h	灰、灰黑色致密状、气孔状伊丁玄武岩、橄榄玄武岩
中生界	白垩系	下统	固阳组		K_1g	灰色砾岩、砂砾岩夹泥岩、黑色泥岩夹煤层, 含大量植物化石
			白音高老组		K_1b	流纹质火山集块岩、流纹质角砾岩屑凝灰岩、流纹质岩屑晶屑凝灰岩、流纹岩
	侏罗系	上统	玛尼图组		J_3mn	安山质-粗安质集块岩和集块角砾岩、辉石安山岩、角闪安山岩、安山岩、粗安岩、含火山角砾的安山质角砾熔岩、安山质-粗安质火山角砾岩
古生界	二叠系	下统	三面井组		P_1s^2	中粗粒(含砾)岩屑长石杂砂岩、中细粒岩屑长石杂砂岩、细砂岩质板岩、泥质粉砂岩
					P_1s^1	青灰色、灰黄色�灰岩、炭质板岩、炭质灰岩和生物碎屑灰岩夹青灰色、灰褐色泥质板岩、粉砂质板岩、中细粒岩屑长石砂岩
	志留系	上统	白乃庙组	二段	$S_{3\text{-}4}b^2$	安山质-英安质凝灰岩、火山角砾岩、凝灰质细-粉砂岩、绿片岩、变质安山质凝灰岩、绿帘绿泥片岩、绢云绿泥片岩、绿泥钠长阳起石片岩、白云母石英片岩、灰黑色变质安山岩、变质安山质集块岩
				一段	$S_{3\text{-}4}b^1$	浅灰色英安岩、灰白色流纹岩及红柱石绢云片岩、片理化变质砂岩、绿泥黑云母石英砂岩、二云绿帘石英片岩、斜长变粒岩、绿泥阳起片岩

图幅区内晚古生代侵入岩的侵位时代为中二叠世, 为 I 型花岗岩, 形成于活动大陆边缘构造环境。

综上, 本数据库为该地区的后续地质调查和研究工作提供了基础数据支撑, 发挥科技创新引领作用, 提升了地质调查工作服务重大科学问题、资源安全、经济社会发展和生态文明建设的能力。

6 结论

(1) 内蒙古北柳图庙幅 (K49E011021)1∶50 000 地质图是中国地质调查局新一轮地质调查的探索性图幅, 采用智能化地质填图方法提升成果表达方式, 对区域地质调查特别是智能化地质调查填图起到了示范引领作用。

(2) 以中国地质调查局最新技术要求为标准, 全面系统编制了北柳图庙幅 (K49E011021) 1∶50 000 地质图并建立了空间数据库, 完善并规范了各类地质信息的表达。

(3) 结合前人资料和本次研究成果, 通过野外沉积建造、构造变形序列研究, 结合岩石地区化学及年代学测试资料, 详细填绘了白乃庙岛弧带的物质组成和构造组合特点。明确白乃庙岛弧带在北柳图庙幅区表现为志留纪源自俯冲板片的埃达克岩侵位，同时发育中酸性火山–沉积地层，地层中发育近东西向紧闭褶皱和陡倾劈理带。

表 4　古生代侵入岩演化序列一览表

时代	填图单位	主体岩性	主要分布位置	形状与产状	主要接触关系	LA–ICP–MS锆石U–Pb年龄/Ma
中二叠世晚期	$x\eta\gamma P_2$	肉红色细粒二长花岗岩	温都尔呼特勒—脑干尚达一带	岩基	侵入$zx\beta\eta\gamma P_2$、$zx\psi\beta\gamma\delta P_2$、$P_1s^1$	263.9±1.1
	$zx\eta\gamma P_2$	肉红色中细粒二长花岗岩	温都尔呼特勒-脑干尚达一带	岩基	侵入$zx\beta\eta\gamma P_2$、P_1s^2	
中二叠世早期	$zx\psi\beta\gamma\delta P_2$	灰白色中细粒角闪黑云花岗闪长岩	古日班额博勒者—阿日音乌苏一带	岩基	侵入$zc\gamma\delta o S_3$、$z\gamma\delta o S_3$、P_1s^1	268.4±1.6
	$zx\pi\delta o P_2$	灰白色中细粒斑状石英闪长岩	包哈音沃博勒者、阿日音乌苏附近	岩基	侵入$zx\gamma\delta o S_3$、$z\gamma\delta o S_3$、P_1s^1	
晚志留世	$z\pi\gamma\delta o S_3$	灰白色中粒斑状英云闪长岩	苏吉—乌泥脑包一带	岩基	侵入$zx\gamma\delta o S_3$, 被$x\eta\gamma P_2$、侵入	423.1±1.5
	$zx\pi\gamma\delta o S_3$	灰白色中细粒斑状英云闪长岩	苏吉—乌泥脑包一带	岩基	侵入$zx\gamma\delta o S_3$, 被$x\eta\gamma P_2$侵入	
	$zc\gamma\delta o S_3$	灰白色中粗粒英云闪长岩	哈日敖包—乌日舍勒图一带	岩基	被$z\pi\gamma\delta o S_3$、$zx\pi\gamma\delta o S_3$侵入, 侵入$zx\beta\gamma\delta S_1$	425.8±1.6
	$z\gamma\delta o S_3$	灰白色中粒英云闪长岩	哈日敖包—乌日舍勒图一带	岩基	被$z\pi\gamma\delta o S_3$、$zx\pi\gamma\delta o S_3$侵入, 侵入$zx\beta\gamma\delta S_1$	434.2±2.2
	$zx\gamma\delta o S_3$	灰白色中细粒英云闪长岩	哈日敖包—乌日舍勒图一带	岩基	被$z\pi\gamma\delta o S_3$、$zx\pi\gamma\delta o S_3$侵入, 侵入$zx\beta\gamma\delta S_1$	
晚寒武世	$x\gamma gn\epsilon_3$	灰白色细粒含石榴白云母花岗岩	毕鲁图庙西北角出山口西侧	岩枝	被$z\gamma\delta o S_3$侵入, 与白乃庙群为断层接触	500.8±2.4

注：x表示细粒; z表示中粒; zc表示中粗粒; zx表示中细粒。

表 5　内蒙古北柳图庙幅（K49E011021）地质图空间数据库测试分析数据表

数据类型	数据量	数据基本特征
岩石化学分析数据	176件	火山岩、侵入岩的11种主量元素
微量元素分析数据	176件	火山岩、侵入岩的31种微量元素
同位素年龄数据	10件	火山岩、侵入岩、碎屑岩的LA–ICP–MS锆石U-Pb同位素年龄

(4) 对北柳图庙幅区志留系、二叠系、白垩系等沉积建造类型、岩浆岩、构造变形序列进行了重新划分与厘定, 并构建了相对完善的构造演化序列。系统建立了白乃庙古生代地质体的沉积建造、构造组合样式与时代属性。将原划为奥陶纪的早古生代岛弧侵入岩重新厘定为志留纪, 锆石 U–Pb 同位素年龄为 414.4 ~ 434.2 Ma。图幅内晚古生代侵入岩集中于中二叠世侵位，具有陆缘弧花岗岩特征。

致谢：内蒙古北柳图庙幅 1∶50 000 地质图是一项集体成果, 项目组一线地质工作人员付出了辛勤的努力。在地质图填绘及数据库的建立过程中, 得到多位填图科学家的辛勤指导, 在此对各位专家和野外项目组所有成员表示最诚挚的感谢。

注释:

❶ 内蒙古自治区地质局区域地质测量队. 内蒙古自治区镶黄旗幅 1∶20 0000 区域地质测量报告.

1976.

❷ 内蒙古地质矿产勘察院. 内蒙古自治区锡林郭勒盟太古生庙等四幅 1∶50 000 矿调地质报告. 2008.

❸ 中化地质矿山总局内蒙古地质勘查院. 内蒙古自治区阿拉善盟风化梁等四幅 1∶50 000 区域矿产地质调查报告. 2012.

❹ 内蒙古自治区地质调查院. 内蒙古查干哈达庙——别鲁乌图地区矿产远景调查报告. 2012.

参考文献

Allen M B, Windley B F, Zhang C. 1993. Palaeozoic collisional tectonics and magmatism of the Chinese Tien Shan, Central Asia[J]. Tectonophysics, 220(1–4): 89−115.

Allen M B, Engor A M C, Natalin B A. 1995. Junggar, Turfan and Alakol basins as Late Permian to Early Triassic extensional structures in a sinistral shear zone in the Altaid orogenic collage. Central Asia[J]. Journal of the Geological Society (London), 152(2): 32−338.

Coleman R G. 1989. Continental growth of Northwest China[J]. Tectonics, 8(3): 621−635.

Gao J, Li M S, Xiao X C, Tang Y Q, He G Q. 1998. Paleozoic tectonic evolution of the Tianshan orogen, northwestern China[J]. Tectonophysics, 287(1–4): 213−231.

Han B F, He G Q, Wang X C, Guo Z J. 2011. Late Carboniferous collision between the Tarim and Kazakhstan-Yili terranes in the western segment of the South Tian Shan Orogen, Central Asia, and implications for the Northern Xinjiang, western China[J]. Earth Science Reviews, 109: 74−93.

Jahn B M, Griffin W L, Windley B F. 2000. Continental growth in the Phanerozoic: Evidence from Central Asia[J]. Tectonophysics, 328(1): vii−x.

Jian P, Liu D Y, KrNer A, Windley B F, Shi Y, Zhang F Q, Shi G H, Miao L C, Zhang W, Zhang Q, Zhang L Q, Ren J S. 2008. Time scale of an early to mid-Paleozoic orogenic cycle of the longlived Central Asian Orogenic Belt, Inner Mongolia of China: implications for continental growth[J]. Lithos, 101(3–4): 233−259.

Li Y L, Zhou H, Brouwer F M, Xiao W, Wijbrans J R, Zhong Z. 2014. Early paleozoic to middle triassic bivergent accretion in the Central Asian Orogenic Belt: insights from zircon U-Pb dating of ductile shear zones in central Inner Mongolia, China[J]. Lithos, 205(9): 84−111.

Li Y J, Wang G H, Santosh M, Wang J F, Dong P P, Li H Y. 2018. Supra-subduction zone ophiolites from Inner Mongolia, North China: Implications for the tectonic history of the southeastern Central Asian Orogenic Belt[J]. Gondwana Research, 59: 126−143.

Li Y J, Wang G H, Santosh M, Wang J F, Dong P P, Li H Y. 2020. Subduction initiation of the SE Paleo-Asian Ocean: Evidence from a well preserved intra-oceanic forearc ophiolite fragment in central Inner Mongolia, North China[J]. Earth and Planetary Science Letters, 535: 116087.

Liu M, Zhang D, Xiong G Q, Zhao H T, Di Y J, Wang Z, Zhou Z G. 2016. Zircon U–Pb age Hf isotope and geochemistry of Carboniferous intrusions from the Langshan area, Inner Mongolia: Petrogenesis and tectonic implications[J]. Journal of Asian Earth Sciences, 120: 139−158.

Liu Y J, Li W M, Feng Z Q, Wen Q B, Franz Neubauer, Liang C Y. 2017. A review of the Paleozoic tectonics in the eastern part of Central Asian Orogenic Belt[J]. Gondwana Research, 43: 123−148.

Sengor A M C, Natalin B A, Burtman V S. 1993. Evolution of the Altaid tectonic collage and Palaeozoic crustal growth in the Eurasia[J]. Nature, 364: 299−304.

Windley B F, Allen M B, Zhang C, Zhao Z Y, Wang G R. 1990. Paleozoic accretion and Cenozoic redeformation of the Chinese Tien Shan range, Central Asia[J]. Geology, 18(2): 128−131.

Windley B F, Alexeiev D, Xiao W J, Kröner A. 2007. Badarch G. Tectonics models for accretion of the Central Asian Orogenic Belt[J]. Journal of Geological Society, 164: 31−47.

Xiao W J, Windley B F, Hao J, Zhai M. 2003. Accretion Leading to Collision and the Permian Solonker Suture, Inner Mongolia, China: Termination of the Central Asian Orogenic Belt[J]. Tectonics, 22(6): 1069−1090.

Xiao W J, Windley B F, Badarch G, Sun S, Li J L, Qin K Z, Wang Z H. 2004. Palaeozoic accretionary and convergent tectonics of the southern Altaids: Implications for the growth of Central Asia[J]. Journal of the Geological Society, 161(3): 339−342.

Xiao W J, Mao Q G, Windley B F, Han C M, Qu J F, Zhang J E, Ao S J, Guo Q Q, Cleven N R, Lin S F, Shan Y H, Li J L. 2010. Paleozoic multiple accretionary and collisional processes of the Beishan orogenic collage[J]. American Journal of Science, 310: 1553−1594.

Xu B, Charvet J, Chen Y, Zhao P, Shi G Z. 2013. Middle Paleozoic convergent orogenic belts in western Inner Mongolia (China): framework, kinematics, geochronology and implications for tectonic evolution of the Central Asian Orogenic Belt[J]. Gondwana Research, 23(4): 1342−1364.

Xu B, Zhao P, Wang Y Y, Liao W, Luo Z W, Bao Q Z, Zhou Y H. 2015. The pre-Devonian Tectonic Framework of Xing'an–Mongolia Orogenic Belt (XMOB) in North China[J]. Journal of Asian Earth Sciences, 97(Part B): 183−196.

Xu Z, Han B F, Ren R, Zhou Y Z, Zhang L, Chen J F, Su L, Li X H, Liu D Y. 2012. Ultramafic-mafic mélange, island arc and post-collisional intrusions in the Mayile Mountain, West Junggar, China: implications for Paleozoic intraoceanic subduction-accretion process[J]. Lithos, 132–133: 141−161.

Yuan Y, Zong K Q, He Z Y, Klemd R, Jiang H Y, Zhang W, Liu Y S, Hu Z C, Zhang Z M. 2018. Geochemical evidence for Paleozoic crustal growth and tectonic conversion in the Northern Beishan Orogenic Belt, southern Central Asian Orogenic Belt[J]. Lithos, 302–303: 189−202.

Zhang W, Jian P, Kröner A, S hi, Y R. 2013. Magmatic and metamorphic development of an early to mid-Paleozoic continental margin arc in the southernmost Central Asian Orogenic Belt, Inner Mongolia, China[J]. Journal of Asian Earth Sciences, 72: 63−74.

Zhang X H, Gao Y L, Wang Z J, Liu H, Ma Y G. 2012. Carboniferous appinitic intrusions from the northern North China craton: geochemistry, petrogenesis and tectonic implications[J]. Journal of the Geological Society, 169: 337−351.

白瑾. 2003. 造山带构造样式的恢复及其构造环境意义 [J]. 地质调查与研究, 26(1): 38−44.

柳长峰, 刘文灿, 王慧平, 周志广, 张华锋, 唐永举. 2014. 华北克拉通北缘白乃庙组变质火山岩锆石定年与岩石地球化学特征 [J]. 地质学报, 88(7): 1273−1287.

刘洋, 滕飞, 王文龙, 杨泽黎. 2020. 内蒙古北柳图庙幅 1：50 000 地质图数据库 [DB/OL]. 地质科学数据出版系统. (2020-06-30). DOI:10.35080/data.A.2020.P7.

李俊建, 党智财, 赵泽霖, 石玉若, 刘敦一, 李超, 屈文俊, 王存贤, 付超, 唐文龙, 张彤, 王守光, 周红英,

赵丽君, 刘晓雪. 2015. 内蒙古白乃庙铜矿床成矿时代的研究 [J]. 地质学报, 89(8): 1448−1457.

钱筱嫣, 张志诚, 陈彦, 于海飞, 罗志文, 杨金福. 2017. 内蒙古朱日和地区早古生代岩浆岩年代学、地球化学特征及其构造意义 [J]. 地球科学, 42(9): 1472−1494.

王树庆, 胡晓佳, 赵华雷. 2019. 内蒙古苏左旗洪格尔地区新发现晚石炭世碱性花岗岩 [J]. 地质调查与研究, 42(2): 81−85.

吴飞, 张拴宏, 赵越, 叶浩. 2014. 华北地块北缘内蒙古固阳地区早二叠世岩体的侵位深度及其构造意义 [J]. 中国地质, 41(3): 824−837.

张维, 简平. 2012. 华北北缘固阳二叠纪闪长岩–石英闪长岩–英云闪长岩套 HSRIMP 年代学 [J]. 中国地质, 39(6): 1593−1603.

赵闯, 苏旭亮, 薛斌, 程东江, 史兴俊, 宋涛涛, 张阔. 2020. 内蒙古西部苦楚乌拉–英巴地区花岗岩锆石 U–Pb 定年及地球化学特征 [J/OL]. 中国地质, 1-22[2020-07-07]. http://kns.cnki.net/kcms/detail/11.1167.P.20200210.2231.004.html.

赵磊, 牛宝贵, 徐芹芹, 杨亚琦. 2019. 新疆东准噶尔卡拉麦里蛇绿岩带两侧志留–石炭系沉积和构造特征分析及其意义 [J]. 中国地质, 46(3): 615−628.

赵越, 陈斌, 张拴宏, 刘建民, 胡健民, 刘健, 裴军令. 2010. 华北克拉通北缘及邻区前燕山期主要地质事件 [J]. 中国地质, 37(4): 900−915.

doi: 10.12029/gc2020Z107

Article Citation: Liu Yang, Teng Fei, Wang Wenlong, Yang Zeli, Wang Shuqing, Hu Xiaojia, Guo Shuo, He Peng. 2020. 1∶50 000 Geological Map Database of Beiliutumiao Map-sheet, Inner Mongolia[J]. Geology in China, 47(S1):86−105.

Dataset Citation: Liu Yang; Teng Fei; Wang Wenlong; Yang Zeli. 1∶50 000 Geological Map Database of Beiliutumiao Map-sheet, Inner Mongolia(V1). Tianjin Center, China Geological Survey[producer], 2016. National Geological Archives of China[distributor], 2020-06-30. 10.35080/data.A.2020.P7; http://dcc.cgs.gov.cn/en//geologicalData/details/doi/10.35080/data.A.2020.P7.

Received: 26-04-2020
Accepted: 09-06-2020

Fund Project:
Funded by China Geological Survey Project "Regional Geological Survey in Wenduermiao-Xianghuang Banner Area, Inner Mongolia (No.DD20190038)"

1∶50 000 Geological Map Database of Beiliutumiao Map-sheet, Inner Mongolia

LIU Yang, TENG Fei*, WANG Wenlong, YANG Zeli, WANG Shuqing, HU Xiaojia, GUO Shuo, HE Peng

(*Tianjin Center*, *China Geological Survey*, *Tianjin* 300170, *China*)

Abstract: According to the '*Technical Requirement for Regional Geological Survey* (*1∶50 000*)' (DD 2019–01) and other uniform standards and requirements, and making full use of the data for 1∶200 000 regional geological and 1∶50 000 mineral survey, the 1∶50 000 Geological Map of Beiliutumiao Map-sheet (K49E011021), Inner Mongolia was compiled by adopting the *Digital Geological Survey System* (DGSS) in combination with Spot, ETM, Aster and other remote sensing images to continuously verify and modify tectonic and lithologic boundaries. As an achievement with important value of reference in the Wenduermiao-Bainaimiao area of Inner Mongolia, the map provides detailed information on the rock composition and tectonic association of the Bainaimiao island-arc belt. We re-divide sedimentary formation into different types, i.e., Silurian, Permian, Cretaceous, and classify intrusive rocks in the region into four phases, establishing a relatively complete tectonic evolutionary series. The map database includes three informal mapping units, 10 formal stratigraphic units, four periods of magmatic events and two tectonic deformations, as well as the whole rock analysis of 176 samples, and zircon U–Pb ages of 10 samples, with a data size of 28.9 MB. The map details the tectonic and magmatic evolution process of the Bainaimiao subduction belt formed in the southward subduction of the Wenduermiao tectonic belt in the north. Reflecting the latest results of the 1∶50 000 regional geological survey, the database holds important scientific value regarding the Paleozoic tectonic evolution of the Wenduermiao orogenic belt. It may also serve as an important reference for subsequent geological surveys in the region. As the first pilot map of China Geological Survey to apply comprehensive regional geological survey mapping, the present project represents the first time to realize whole-

About the first author: LIU Yang, male, born in 1986, master, engineer, mainly engages in structural geology and regional geological survey; E-mail: 12531376@qq.com.

The corresponding author: TENG Fei, male, born in 1987, master, engineer, mainly engages in regional geological survey; E-mail: 267272916@qq.com.

process field investigation in China's regional geological surveys.

Key words: Inner Mongolia; Beiliutumiao Map-sheet; 1：50 000; geological map; database; Xing'an-Mongolia orogenic belt; geological survey engineering
Data service system URL: http://dcc.cgs.gov.cn

1 Introduction

The Xing'an-Mongolia orogenic belt has recorded a large amount of important information such as the subduction of the Paleo-Asian Ocean, the collision of the Siberia plate and North China plate (Xiao WJ et al., 2003; Jian P et al., 2008; Xu B et al., 2015). Its tectonic evolution process is closely related to tectonic movement of the Paleo-Asian Ocean (Windley BF et al., 2007; Han BF et al., 2011; Xu Z et al., 2012; Zhang XH et al., 2012; Wang SQ et al., 2019; Zhao Y et al., 2010). The process of subduction-accretion orogeny and suturing of terranes has resulted in the existing framework of the Xing'an-Mongolia orogenic belt (Coleman RG, 1989; Windley BF et al., 1990; Allen MB et al., 1993, 1995; Sengor AMC et al., 1993; Gao J et al., 1998; Jahn BM et al., 2000; Windley BF et al., 2007; Xiao WJ et al., 2004, 2010; Li YJ et al., 2018, 2020; Yuan Y et al., 2018; Zhao L et al., 2019; Zhao C et al., 2020). A correct understanding of the evolution of the Xing'an-Mongolia orogenic belt is of great significance to restoring the tectonic history of the central Asian orogenic belt (CAOB). In recent years, a large number of scientific studies have been conducted on important geological issues in the northern margin of the North China plate, obtaining abundant data (Wu F et al., 2014; Zhang W et al., 2012; Zhang W et al., 2013; Liu M et al., 2016). At present, most scholars believe that the Paleo-Asian Ocean experienced a two-way subduction on the north and south sides in the Early Paleozoic (Xu B et al., 2013; Li YL et al., 2014; Liu YJ et al., 2017), forming two corresponding island-arc subduction zones (Jian P et al., 2008), of which the southern subduction zone, located in the Bateaobao–Bainaimiao–Winduermiao region, has relatively complete subduction records and includes the Wenduermiao subduction-accretionary complex and the Bainaimiao island-arc igneous rock belt.

The area of the 1：50 000 Geological Map of Beiliutumiao Map-sheet, Inner Mongolia is located on the Bainaimiao island-arc igneous rock belt originating from the southern subduction belt to the north of the northern margin of the North China plate (Fig. 1). The regional geological survey of Xianghuang Banner Map-sheet (1：200 000)[1] was first carried out in 1976 by the regional geological survey team of the Geology and Mineral Resource Bureau of Inner Mongolia Autonomous Region, with complete and systematic review of the stratigraphic framework, magmatic activity and tectonic evolution in the area. In 2008, the Geology and Mineral Exploration Institute of Inner Mongolia completed four 1：50 000 geological and mineral surveys[2], including Taigushengmiao in Xilingol League, Inner Mongolia. In 2012, the Inner Mongolia Geological Exploration Institute of China Chemical Geology and Mine Bureau completed four 1：50 000 regional mineral geological surveys[3] in the Temurtei area of Ulanqab City, Inner Mongolia. The Geological Survey Institute of Inner Mongolia has completed a survey of mineral prospects in the Chaganhadamiao-Bieluwutu

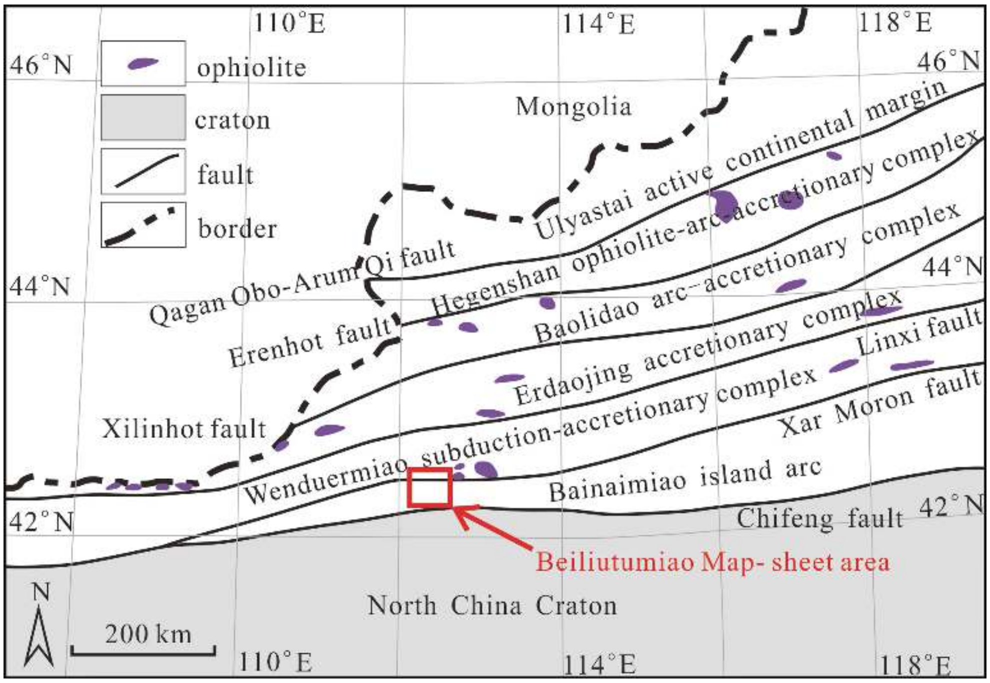

Fig. 1 Geotectonic location of Beiliutumiao map-sheet (K49E011021), Inner Mongolia (modified from Xiao WJ et al., 2003)

region of Inner Mongolia[4]. In addition, in recent years, a large number of scientific studies have been conducted and rich data have been accumulated revolving around the Paleozoic evolution of the Wenduermiao orogenic belt (Liu CF et al., 2014; Li JJ et al., 2015; Qian XY et al., 2017). These studies have laid a solid foundation for the compilation of the geological map of the Beiliutumiao Map-sheet.

The 1：50 000 Geological Map of Beiliutumiao Map-sheet represents a pilot project of regional geological survey mapping. It aims to describe in detail the Paleozoic tectonic evolution of the Bainaimiao island-arc belt with objectively expressed field geological facts by incorporating previous geological surveys, mineral exploration and latest research results, by adopting advanced mapping approaches and geological mapping methods combined with tectonic analysis of the orogenic belt (Bai J, 2003). The 1：50 000 Geological Map Database (Table 1, Liu Y et al., 2020) of Beiliutumiao Map-sheet, Inner Mongolia systematically reflects the attributes of sedimentary formation, tectonic association and eras of Bainaimiao Paleozoic geobodies, thus providing useful reference materials for geological research and field geological surveys in the Wenduermiao area.

2 Data Acquisition and Processing Methods

2.1 Data Source

In line with the '*Technical Requirement for 1：50 000 Regional Geological Survey*' (DD 2019–01) and based on the original data (including geological sketches and remote sensing interpretation images) of the 1：50 000 mineral geological survey project, the 1：50 000 Geological Map of Beiliutumiao Map-sheet, Inner Mongolia is created according to actual field

Table 1 Metadata Table of Database (Dataset)

Items	Description
Database (dataset) name	1：50 000 Geological Map Database of Beiliutumiao Map-sheet, Inner Mongolia
Database (dataset) authors	Sedimentary rocks: Liu Yang, Tianjin Center, China Geological Survey Volcanic rocks: Teng Fei, Tianjin Center, China Geological Survey Igneous rocks: Wang Wenlong, Tianjin Center, China Geological Survey Metamorphic Rocks: Yang Zeli, Tianjin Center, China Geological Survey
Data acquisition time	2016—2018
Geographic area	113°00′–113°30′ E, 42°00′–42°20′ N
Data format	MapGIS
Data size	28.9 MB
Data service system URL	http://dcc.cgs.gov.cn
Fund project	China Geological Survey project named “Regional Geological Survey in Wenduermiao-Xianghuang Banner Area, Inner Mongolia” (DD20190038)
Language	Chinese
Database (dataset) composition	The 1：50 000 Geological Map Database of Beiliutumiao Map-sheet includes: 1：50 000 geological map, mosaic maps and map decorations. The geological map includes sedimentary rocks, volcanic rocks, intrusive rocks, Quaternary, structural feature, geological boundary, attitude, mineralized spot, alteration, lithological pattern and various codes. The mosaic maps include comprehensive stratigraphic columns, intrusive rock mapping units, map cross sections and geotectonic locations. Map decorations include map sheet indices, legends of master maps, an author information table

data (actual material map and section map). It represents the latest 1：50 000 geological mapping result of the Beiliutumiao Map-sheet. Its geographical base maps adopt the latest geographic data of National Geomatics Center of China (NGCC) and applies existing technical standards and computer software such as *Digital Geological Survey System* (DGSS) and MapGIS for data processing.

2.2 Data Processing

2.2.1 Pre-research Database

The pre-research database includes various remote sensing images, satellite images, geophysical and geochemical exploration maps. After being validated, the images are calibrated and projected to a 1：50 000 standard frame and digital topography. Gauss-Kruger projection is adopted for field base maps and China Geodetic Coordinate System 2000 (CGCS 2000) is adopted for data samples. Geological sketches are compiled by incorporating the data of the 1:200 000 geological map and the 1：50 000 mineral geological map. All sub-map numbers and rock codes are standardized according to the ‘*Legend of 1：50 000 Regional Geological Map’* (GB 958—99). Work is deployed on this basis, and field mapping units are preliminarily divided based on the lithostratigraphic clearing in Inner Mongolia and previous research results to compile a dictionary database for digital mapping so as to provide reference for field geological surveys.

2.2.2 Field Original Database

Based on the comprehensive analysis of the existing data and geological sketches, we established key working areas and general working areas, and identified volcanic rocks and igneous rocks in the Bainaimiao island-arc as the key contents of mapping, and densely deployed routes in complex areas. The original database as a whole can be divided into digital mapping data and digital section databases.

Digital mapping is based on a 1：25 000 base map. Through actual route survey in the field, we collected information on geological spots, geological boundaries and geological routes in the digital mapping system. Information such as the properties of different spots, lithology, and attitude were observed and entered to form free hand field maps. The free hand field map library stores various types of data of geological routes, and represent the most important first-hand original database. After having checked the free hand field map database for accuracy, all contents of geological routes were entered into the library and integrated to form a field PRB general library, and the physical observation data point, line layer and label layer were further inherited into the actual material library. In general, free hand field maps were processed through the following steps:

(1) Standardized processing of free hand field maps: imported map data collected in the field into the computer, and supplement and refine the contents regarding geological spot (P), geological route (R), geological boundary (B), attitude, sampling, photo and attribute, while maintaining overall coordination and consistency to ensure objective and accurate description.

(2) Finishing processing of free hand field maps: adopt topography and remote sensing data in drawing boundaries. Regarding the “V-shaped” route, boundaries on both sides must correspond to each other. On this basis, processing shall be carried out to meet requirements for line type, sub-map number and color, with smooth finishing, and lithological annotation added between spots to facilitate subsequent mapping.

(3) Comprehensive arrangement of free hand field maps: summarize field routes for each task, systematically process information on strata and igneous rocks, with special treatment of contact relation and tectonic deformation, and conduct data quality inspection and self-check before submission for mapping.

The digital section database is developed by means of digital cross section survey. Taking the free hand field maps as the base maps, and on the basis of full geological reconnaissance, we selected sections with complete outcrops and recorded information regarding lithology, sample, attitude, photo and tectonic deformation in a layer-by-layer approach, and drew cross section sketches based on field notes, which were stored with automatically generated document names or customized file names as needed. In general, after the complete cross section is measured, the section recorder would carry out preliminary processing of the section and make a brief summary of field work, and draw section maps and column maps while taking indoor slice identification results into account.

2.2.3 Actual Material Maps

The actual material maps represent important original data using spatial entities including points, lines and planes to represent the density of distribution of various geological elements such as geological spots, geological boundaries, segmented routes, geobodies, samples, attitude, and GPS points. In principle, 1∶25 000 map-sheets are required for the original data of the 1∶50 000 regional geological survey, including actual material maps. Free hand field maps were arranged with the following steps:

(1) Formation of geobody boundary. The file name of the line layer used for mapping in the actual material library is Geoline.wl. To establish topological relation and form geobody surface, in addition to geobody boundary line, the file includes internal map frame lines, planar water bodies, snowy mountains, deserts and other boundaries, of which the latter were directly copied from relevant map layers. Note: Finishing boundaries that do not divide geobody surfaces were not classified into Geoline.wl layers, such as some lithofacies boundaries, unconfirmed remote sensing images of faults, and metamorphic facies zones.

(2) Formation of geobody surface. After the formation of geobody boundaries, geobody surface entities can be formed through topology. Topological reconstruction and error checking were carried out mainly through the line-arc sections of geobodies. The newly generated temporary area file had no attribute structure and was merged into the geobody area file of the actual material library.

(3) Attribute assignment. After the line and surface files of digital material maps were formed and assigned attribute structure, it is necessary to supplement and refine their content, including extraction of geobody boundary attributes, extraction of geobody surface entity attributes, assigning geobody codes on the left and right sides of the boundary according to geobody surface, and browsing and editing actual material map attributes.

(4) The arrangement of actual material maps includes uniform coloring of different geobodies according to their attributes, modification of different types of geobody boundary lines and corresponding parameters in line with relevant standards and specifications, annotation of different geobody codes according to requirement, and finishing of the map border, with an emphasis on refinement of the legend. Useless empty files automatically generated by the system were deleted from the map library.

2.2.4 Original Drawing

The original manuscript is equivalent to the geological map. The 1∶50 000 original map was formed on the basis of the 1∶25 000 actual material map, after which normative and standardized processing is needed. Specifically, it includes the processing of geobody boundary layer, geobody surface layer, attitude layer, geological map finishing layer, geobody labeling, off-map finishing layer, original library files and other layers and documents. Useless empty files automatically generated by the system were deleted from the map library. Field geological layer files were deleted from the original engineering files, and only the layer files related to the geological map were kept.

2.2.5 Spatial Database

The spatial database includes several categories, including basic element, comprehensive element, object and independent element, among which element database is a collection of elements sharing the same spatial reference system, and is composed of geological spot, surface and line entities in the geological map data model. In the geological map data model, generally one element category corresponds to multiple object categories. Basic element, comprehensive element and object have complete data item attributes.

The database constructs its graphic database and attribute database in conformity with ‘*Digital Geological Map Layer and Attribute File Format*’ (D/Z 0197—1997) among other standards, and determines the expressions of color, map decorations, legend and symbols according to ‘*Standard and Principle for Coloration of Geological Map*’ (DZ/T 0179—1997) and ‘*Geological Symbols Used for Regional Geological Maps*’ (GB 958—99).

2.2.6 Preparation of Various Mosaic maps

The main mosaic maps of the 1：50 000 Geological Map of Beiliutumiao Map-sheet (K49E011021), Inner Mongolia include: comprehensive stratigraphic column, intrusive rock mapping unit, map cross section, geotectonic location map and other mosaic maps (Fig. 2).

(1) Comprehensive stratigraphic column: the characteristics of sedimentary formations of different lithostratigraphic units were expressed in detail, and the characteristics of stratigraphic sequence and rock association of various stratigraphic units in the map were systematically processed to comprehensively reflect their sedimentary background and era attributes in combination with zircon dating.

(2) Intrusive rock mapping unit: four magmatic evolutionary series have been identified: ① subduction rocks (about 500 Ma) represented by grey-white fine-grained garnet-bearing gneissic muscovite granite in the Late Cambrian; ② the late Silurian is dominated by medium-coarse-grained, medium-grained, and medium-fine-grained tonalite (425 Ma), and medium-grained and medium-fine-grained porphyry tonalite (423 Ma), representing the rock combination of an Early Paleozoic island-arc tectonic setting; ③ the early Middle Permian was

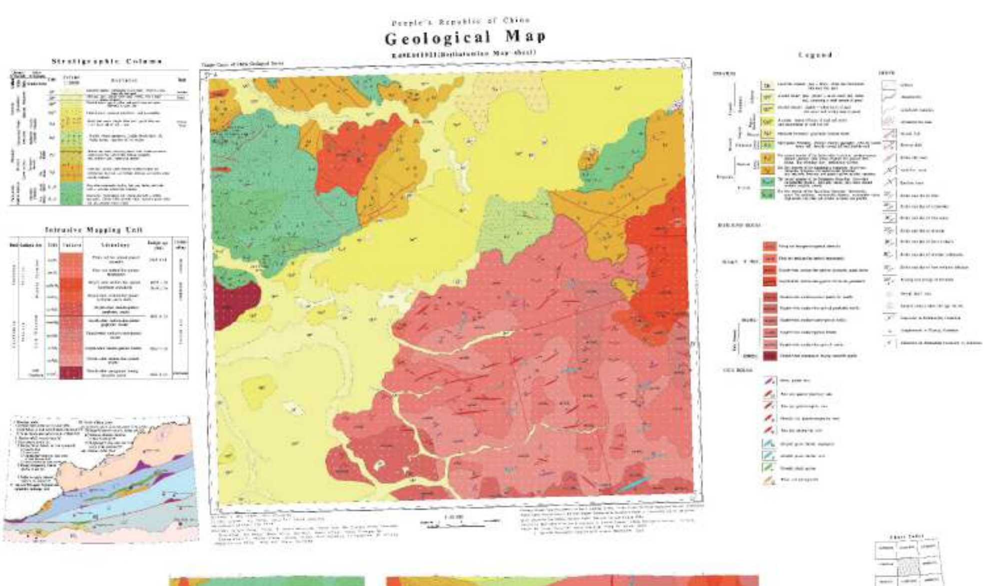

Fig. 2 Schematic diagram of 1: 50 000 geological map of Beiliutumiao map-sheet (K49E011021), Inner Mongolia

dominated by medium-fine-grained quartz diorite and medium-fine-grained granodiorite (about 268 Ma), representing a compressive tectonic setting in the early stage of the Middle Permian; ④ the late stage of the Middle Permian was dominated by monzonitic granite (medium-grained and medium-fine-grained) (about 263 Ma), representing the conversion of a tectonic setting from compressive to extensional.

(3) Map cross section: the general strike of the formation and structure in the map is near-NW-NW. To visually display the contact relation and spatial position of geobodies in the region, two map sections are arranged to comprehensively control the contact relation of geobodies across the map-sheet: ① the large-scale section of Early Paleozoic island-arc volcanic rocks, combined with large-scale tectonic analysis, reflects in detail the material composition and tectonic sequence of Early Paleozoic island-arc volcanic rocks; ② the cross section is arranged in the north-west direction and mainly controls the spatial position of granite and other geobodies in the whole Paleozoic.

(4) Geotectonic location map: it represents the location of the Beiliutumiao Map-sheet in terms of regional geotectonics, and the division of geotectonic units. The geotectonic location map reflects the tectonic location of the trench-arc-basin system formed by the southward subduction of the Early Paleozoic Wenduermiao Ocean and the working area.

(5) Other mosaic maps: dike rocks, geological codes, geological symbols and lithological pattern, and compile legends and table of responsibility.

3 Data Sample Description

3.1 Data Naming Method

Geological surface.wp, geological line.wl, geological spot.wt.

3.2 Layer Content

The main map includes sedimentary rock, volcanic rock, intrusive rock, Quaternary System, structural feature, geological boundary, attitude, and various codes.

The mosaic map includes the comprehensive stratigraphic column, intrusive rock mapping unit, map cross section, and geotectonic location map.

Map decorations include charts, legends, and table of responsibility.

3.3 Data Type

Entity type name: dot, line and surface.

Point entities: symbols and marks of various geobodies, geological patterns, mineralization and alteration;

Line entity: fracturing structure, geological boundary, lithofacies boundary, tectonic boundary, and patterns for special marker layer;

Surface entity: sedimentary rock, volcanic rock, metamorphic rock, intrusive rock, Quaternary System.

3.4 Data Attribute

The 1：50 000 Geological Map Database of Beiliutumiao Map-sheet contains information on geological entity element, geographical element and finishing element. The geographical element attribute is given according to the data attribute structure provided by National Geomatics Center of China (NGCC). The geological entity element attribute is divided into four major rock types according to the requirements for special geological database construction of the 1：50 000 regional geological survey, namely, sedimentary rock, volcanic rock, intrusive rock, and metamorphic rock, fracturing structure, attitude elements, and mineral area, with separately established database attributes.

The attribute of sedimentary rock formation includes: chronostratigraphic unit, lithostratigraphic unit, formation name, formation code, lithologic combination, stratigraphic era, formation thickness, ore-bearing, rock structure, sedimentary structure, rock color, type of sedimentation, sedimentary facies type, and synsedimentary structure.

The attribute of volcanic rock formation includes: chronostratigraphic unit, lithostratigraphic unit, formation name, formation code, stratigraphic age, stratigraphic division, lithologic association, formation thickness, ore-bearing, volcanic eruption cycle, volcanic eruption type, genetic type of volcanic rock, special lithologic interlayer, volcanic rock facies type, and isotope age.

The attribute of intrusive rock formation includes: formation name, formation code, lithologic combination, ore-bearing, rock structure, intrusion stage, rock mass attitude, plane morphology, section morphology, emplacement structure of rock mass, contact zone characteristics, genetic type, and isotopic age.

The attribute of metamorphic rock includes: chronostratigraphic unit, lithostratigraphic unit, formation name, formation code, lithologic combination, stratigraphic age, formation thickness, ore-bearing, rock structure, rock fabric, protolith formation, metamorphic facies, and metamorphic type.

The attribute of fracturing structure includes: fracture name, fracture type, fracture extension, fracture elongation, fracture width, strike, surface dip, surface dip angle, fracture distance, surface shape, tectonic rock characteristics, movement mode, active period, and mechanical properties.

The attribute of attitude includes: attitude type, dip, and dip angle.

See Table 2 for the attribute list of each data item of the basic element category, comprehensive element category and object category of the geological map.

4 Data Quality Control and Evaluation

Overall, field mapping is carried out in conformity with the accuracy standard of the '*Technical Requirement for Regional Geological Survey* (*1：50 000*)' (DD 2019–01). In the actual mapping process, we implemented the key requirements in the pilot draft of the 'T*echnical Requirement for Regional Geological Survey* (*1：50 000*)' (DD 2019–01) issued by China Geological Survey, and adopted intensive route deployment for the bedrock area, and remote sensing interpretation supplemented by field verification for the Mesozoic–Cenozoic stratigraphic area. Routes and tracing routes are intensively deployed in key areas, achieving good results. Geological spot acquisition is based on the principle of fully controlling important contact relations such as geobody boundary, major tectonic boundaries, tectonic deformation, and special lithology.

In the geological mapping of the 1：50 000 Beiliutumiao map-sheet, the field routes of total 385 km were surveyed, together with 993 geological points, 1 702 geological boundaries,

Table 2 Data attribute of the geological map spatial database

Data type	Name	Standard code	Attribute of data item
Basic elemen	Geobody surface	_GeoPolygon	Geobody surface identification number, geobody surface type code, geobody surface name, geobody surface era, lower age limit of geobody surface, upper age limit of geobody surface, sub-type identification
	Geological boundary line	_GeoLine	Element identification number, geological boundary code, geological boundary type, code of geobody on the left side of the boundary, code of geobody on the right side of the boundary, interface strike, interface dip, interface dip angle, sub-type identification
	Attitude	_Attitud	Element identification number, attitude type code, attitude type name, strike, dip, dip angle, sub-type identification
	Sample	_Sample	Element identification number, sample number, sample type code, sample type name, sample rock name, sub-type identification
	Photo	_Photograph	Element identification number, photo number, photo title, photo caption, sub-type identification
	Sketch	_Sketch	Element identification number, sketch number, sketch title, sketch description, sub-type identification
	Fossil	_Fossil	Element identification number, fossil sample number, biological category of fossil, genus or species of fossil, fossil horizon, code number of fossil-bearing stratigraphic unit, fossil era, sub-type identification
	Isotopic dating	_Isotope	Element identification number, sample number, sample name, age determination method, measured age, unit and code of measured geobody, unit conducting measurement and analysis, date of measurement and analysis, sub-type identification
	Crater	_Crater	Element identification number, crater type, crater name, crater size, unit and code of geobody with crater, crater rock type, crater formation era, sub-type identification
	Spring	_Spring	Element identification number, spring type code, spring type name, spring flow rate, spring temperature, unit and code of geobody with spring, sub-type identification
	River, lake, sea and reservoir coastline	_Line_Geograph	Element identification number, map element type, map element name, sub-type identification

Continued table 2

Data type	Name	Standard code	Attribute of data item
Comprehensive element	Tectonic deformation zone	_Tectzone	Element identification number, code of deformation zone, type of deformation zone, deformation zone rock name, structural characteristics of deformation zone, mechanical characteristics of deformation zone, formative era, active period, ore-bearing, sub-type identification
	Altered zone	_Alteration_Polygon	Element identification number, alteration type code, alteration type name, mineral association and content of alteration, ore-bearing, altered geobody code, sub-type identification
	Volcanic facies belt	_Volca_Facies	Element identification number, volcanic lithofacies type and code, stratigraphic unit and code, lithofacies type of volcanic rock, rock structure, rock fabric, flow surface attitude, flowline attitude, formative era, ore-bearing, sub-type identification
	Standard frame (inner frame)	_Map_Frame	Map name, map-sheet code, scale, coordinate system, elevation system, left longitude, lower latitude, graphic unit
Object	Lithostratigraphic unit of sedimentary (volcanic) rock	_Strat	Element category, stratigraphic unit name, stratigraphic unit symbol, stratigraphic unit era, rock association name, main color of rock association, main sedimentary structure of rock formation, biological fossil zone or biological assemblage, stratigraphic thickness, ore-bearing, sub-type identification
	Geochronological unit of intrusive rock	_Intru_Litho_Chrono	Element category, name of rock mass mapping unit, rock mass mapping unit symbol, rock name (lithology), rock color, rock structure, rock fabric, lithofacies, primary minerals and content, secondary minerals and content, contact relation with surrounding rock, surrounding rock era, strike of contact surface with surrounding rock, dip direction of contact surface with surrounding rock, dip angle of contact surface with surrounding rock, attitude of flow surface, attitude of flowline, formative era, ore-bearing, sub-type identification
	Fault	_Fault	Element category code, fault type, fault name, fault number, fault nature, code of hanging wall of fault, code of heading wall of fault, fault fracture zone width, fault strike, fault dip, fault plane dip angle, estimated fault distance, fault formative era, active period and sub-type identification
	Dike rock (face)	_Dike_Object	Dike rock classification code, dike rock name, dike rock symbol, lithology, color, structure, tectonics, main minerals and content, secondary minerals and content, strike of contact surface with surrounding rock, dip direction of contact surface with surrounding rock, dip angle of contact surface with surrounding rock, formative era, ore-bearing property and sub-type identification

Continued table 2

Data type	Name	Standard code	Attribute of data item
	Informal stratigraphic unit	_INF_STRATA	Element category code, informal stratigraphic unit code, lithology, rock structure, biological fossil zone or biological assemblage, outcrop width or thickness, ore-bearing, symbol of stratigraphic unit, sub-type identification
	Planar water area	_Water_Region	Element category code, map element type, map element name, map element feature, sub-type identification
	Basic information of map-sheet	_Sheet_Mapinfo	Topographic map number, map name, scale, coordinate system, elevation system, left longitude, right longitude, upper latitude, lower latitude, mapping method, investigation unit, map acceptance unit, scoring grade, completion time, publication time, data source, data collection date

343 samples for microscopic petrography observation, 176 samples for whole-rock analysis, 10 samples for zircon U–Pb dating, 1 043 photos, the actural measured 1：20 000 stratum profiles of 15 kilometers and 1：50 000 intrusive profiles of about 37 kilometers. The overall accuracy of the mapping meets the specific requirements of the 1：50 000 regional geological special mapping in China.

Generally, only closed geobodies larger than 100 m in diameter, linear geobodies with a width greater than 50 m and a length greater than 250 m, and fault and fold structures with a length greater than 250 m, are represented on the map. Rocks in the ophiolite tectonic mélange belt are appropriately enlarged and expressed by merging similar rocks. Generally, the error between geological spots marked on the free hand field map and their actual positions shall not be greater than 25 m.

In terms of data quality, self-inspection and mutual inspection of mapping routes reached 100%, random inspection by project team reached 30%, which meets relevant quality requirements. The Tianjin Center of China Geological Survey organized experts on October 24, 2016, August 10, 2017 and October 1, 2018 for quality inspection on the progress of the original data and achievements of the project team in the field and indoors. From October 1 to 6, 2018, the Tianjin Center of China Geological Survey organized experts to carry out field work acceptance of the project through a combination of indoor and site inspection. The project was rated as excellent. The final results of four regional geological survey sub-projects, including the 1:50 000 Beiliutumiao Map-sheet, Inner Mongolia, were rated as excellent.

5 Data Value

The 1：50 000 Geological Map of Beiliutumiao Map-sheet (K49E011021), Inner Mongolia is one of the representative maps of the latest geological surveys of China Geological Survey. On the basis of in-depth investigation of rock combinations, sequences and tectonic deformation in this map-sheet, and guided by the latest mapping approaches for orogenic belts, the map is continuously improved in surface structure and layout in conformity with the latest '*Technical Requirement for Regional Geological Survey* (*1：50 000*)' (DD

2019–01). Finally, with Early Paleozoic island-arc structures as its core content, a complete Paleozoic tectonic-magmatic-stratigraphic evolutionary series of the Beiliutumiao area is systematically established based on the analysis of sedimentary formation, magmatic evolutionary series, and tectonic style.

5.1 Characteristics of Sedimentary Formation

In-depth investigation is carried out in the area to identify the material composition, stratigraphic sequence, sedimentary environment and formative era of each stratigraphic unit. The lithostratigraphic framework of the survey area is systematically established, and informal lithostratigraphic units have been mapped. Considering their tectonic setting, we have established the different types of sedimentary formation with detailed description (Table 3). We re-divide the Bainaimiao Formation into two member-level lithostratigraphic units, and identify the material composition, basic sequence, sedimentary environment and deformation and metamorphism characteristics of each unit. The bioclastic limestone, gravelly sandstone and siltstone with Bouma sequence in the Beiliutumiao area are re-classified as Sanmianjing Formation, which is further divided into two lithologic sections. A large number of fusulinid and crinoid fossils have been newly collected from the limestone of the first member of Sanmianjing Formation, providing paleontological basis for chronostratigraphic division. In view of the characteristics of fossil assemblages and regional correlation, we believe that the formative era is the Early Permian.

Table 3 Division of lithostratigraphic mapping units

Chronostratigraphy			Division of lithostratigraphic units	Stratumcode name	Lithologic description
Boundary	System	Series			
Cenozoic	Quaternar System	Holocene	Lacustrine sediment	Qh^{l}	Composed of grey-black, grey-green, sandy silt, clay sand, and gravel.
			Alluvium	Qh^{al}	Located in the modern riverbed, composed of mottled and loosely piled sand and gravel layers, medium sand, and sandy clay.
			Flood alluvium	Qh^{pa}	Mostly forming low and gentle platforms, with deposits being mainly yellow-brown gravel, sand and clay. The gravel is poorly sorted and has complex composition.
		Upper Pleistocene	Flood alluvium	Qp_3^{pal}	The deposits are mainly yellow-brown gravel, sand and clay, poorly sorted and rounded, with complex composition.
	Neogene	Miocene	Hannuoba Formation	N_1h	Grey and grey-black compact, vesicular iddingsite basalt and olivine basalt

Continued table 3

Chronostratigraphy			Division of lithostratigraphic units		Stratumcode name	Lithologic description
Boundary	System	Series				
Mesozoic	Cretaceous	Lower Series	Guyang Formation		K_1g	Grey conglomerate, sandy conglomerate mixed with mudstone, black mudstone mixed with coal seam, rich in plant fossils
			Baiyingaolao Formation		K_1b	Rhyolitic volcanic agglomerate, rhyolitic breccia tuff, rhyolitic crystal tuff, rhyolite
	Jurassic	Upper Series	Manitu Formation		J_3mn	Anesite-trachytic agglomerate and agglomerate breccia, pyroxene andesite, hornblende andesite, andesite, trachyandesite, volcanic breccia-bearing andesitic breccia lava, andesite-trachyandesitic volcanic breccia
Paleozoic	Permian	Lower Series	Sanmianjing Formation		P_1s^2	Medium-coarse-grained (gravelly) lithic feldspar greywacke, medium-fine-grained lithic feldspar greywacke, fine sandstone slate, argillaceous siltstone
					P_1s^1	Blue-grey, grey-yellow fusulinid limestone, carbonaceous slate, carbonaceous limestone and bioclastic limestone mixed with blue-grey, grey-brown argillaceous slate, silty slate, medium-fine-grained lithic feldspathic sandstone
	Silurian System	Upper Series	Bainaimiao Formation	Second Member	$S_{3\text{-}4}b^2$	Andesite-dacite tuff, volcanic breccia, tuff fine-siltstone, chlorite schist, metamorphic andesitic tuff, epidote-chlorite schist, sericite chlorite schist, chlorite-albitite actinolite schist, muscovite quartz-schist, grey-black metamorphic andesite, metamorphic andesitic agglomerate
				First Member	$S_{3\text{-}4}b^1$	Light-grey dacite, grey-white rhyolite and andalusite-sericite schist, schistositized metamorphic sandstone, chloritized biotite quartz-sandstone, two-mica epidote quartz schist, plagioclase granulite, chlorite actinolite schist

5.2 Structural Style Combination Characteristics

The structural framework and deformation sequence are studied in detail, and two periods of fold deformation are identified in the area: the first period of deformation occurred at the end of the Early Paleozoic and was an outcrop-scale buckle compound tight fold formed by a strong contraction-collision structure in the near north-south direction; the second period of fold deformation largely developed after the Late Paleozoic Sanmianjing period and superimposed on the first period of folding, mainly represented by normal-broad folds on a kilometer scale, with strong lamellar intersection and cleavage refraction.

5.3 Evolutionary Series of Intrusive Rocks

Based on the characteristics of field rock combinations and zircon U–Pb dating, the intrusive rocks in the Map-sheet are divided into four eras (Table 4), including the Late Cambrian, the Late Silurian, the early stage of the Middle Permian, and the late stage of the Middle Permian, with the evolutionary series of igneous rocks established.

5.4 Significance of Geochemical Test Data

This database contains geochemical testing and analysis of rocks in the map-sheet area (Table 5), and is able to reflect important information about petrogenesis and diagenetic age, thus providing scientific basis for the study of regional geological background and evolution in the Beiliutumiao area of Inner Mongolia. Early Paleozoic island-arc intrusive rocks, which were previously classified as Ordovician, are re-classified as Silurian adakite originating from subducted oceanic crust, with zircon U–Pb age ranging from 414.4 Ma to 434.2 Ma. The identification of magmatic events in this period indicates that Early Paleozoic subduction in the region has continued to the Late Silurian (~420 Ma), representing constraints for the evolution of the Paleo-Asian Ocean and the Xing'an-Mongolia orogenic belt. The Late Paleozoic intrusive rocks in the map-sheet area is Type I granite formed in the tectonic environment of an active continental margin. Its emplacement age is the Middle Permian.

This database, as a result of scientific innovation, provides basic data support for subsequent geological surveys and research in the region, and improves the ability of geological surveys to answer major scientific questions, ensure resource security, and facilitate the development of society, economy and ecological civilization.

6 Conclusion

(1) The 1：50 000 Geological Map of Beiliutumiao Map-sheet (K49E011021), Inner Mongolia represents an exploratory project of the new round of geological surveys of China Geological Survey. The map adopts geological mapping to improve the expression of results, and plays an exemplary and leading role in regional geological surveys, especially in comprehensive geological survey mapping.

(2) In conformity with the latest technical requirements of China Geological Survey, the 1：50 000 Geological Map of Beiliutumiao Map-sheet (K49E011021) is compiled in a comprehensive and systematic way, with a spatial database established, in which the

Table 4 List of evolutionary sequences of Paleozoic intrusive rock

Era	Mapping unit	Main lithology	Main distribution	Shape and attitude	Main contact relation	LA-ICP-MS zircon U–Pb age/Ma
Late stage of Middle Permian	x*ηγ*P_2	Meat-red fine-grained monzonitic granite	Wenduerhutele-Naoganshangda area	Rock foundation	Intrusion into zx*βηγ*P_2, zx*ψβγδ*P_2, P_1s^1	263.9±1.1
	zx*ηγ*P_2	Meat-red medium-fine-grained monzonitic granite	Wenduerhutele-Naoganshangda area	Rock foundation	Intrusion into zx*βηγ*P_2, P_1s^2	
Early stage of Middle Permian	zx*ψβγδ*P_2	Grey-white medium-fine-grained hornblende biotite granodiorite	Guribanebolezhe-Ariyinwusu area	Rock foundation	Intrusion into zc*γδo*S_3, z*γδo*S_3, P_1s^1	268.4±1.6
	zx*πδo*P_2	Grey-white medium-fine-grained porphyry tonalite	Vicinity of Baohayinwobolezhe, Ariyinwusu	Rock foundation	侵入zx*γδo*S_3、z*γδo*S_3、P_1s^1Intrusion into zx*γδo*S_3, z*γδo*S_3, P_1s^1	
Late Silurian	z*πγδo*S_3	Grey-white medium-grained porphyry tonalite	Suji-Wuninaobao area	Rock foundation	Intrusion into zx*γδo*S_3, intruded by x*ηγ*P_2	423.1±1.5
	zx*πγδo*S_3	Grey-white medium-fine-grained porphyry tonalite	Suji-Wuninaobao area	Rock foundation	Intrusion into *zxγδo*S_3, intruded by x*ηγ*P_2	
	zc*γδo*S_3	Grey-white medium-coarse-grained porphyry tonalite	Hariaobao-Wurisheletu area	Rock foundation	Intruded by z*πγδo*S_3, zx*πγδo*S_3, Intrusion into zx*βγδ*S_1	425.8±1.6
	z*γδo*S_3	Grey-white medium-grained tonalite	Hariaobao-Wurisheletu area	Rock foundation	Intruded by z*πγδo*S_3, zx*πγδo*S_3,intrusion into zx*βγδ*S_1	434.2±2.2
	zx*γδo*S_3	Grey-white medium-fine-grained tonalite	Hariaobao-Wurisheletu area	Rock foundation	Intruded by z*πγδo*S_3, zx*πγδo*S_3, Intrusion into zx*βγδ*S_1	
Late Cambrian	x*γgn*Є$_3$	Grey-white fine-grained garnet-bearing muscovite granite	West side of the northwest corner exit of Bilutumiao	Apophysis	Intruded by z*γδo*S_3; forms fault contact with Bainaimiao Group	500.8±2.4

Note: x denotes fine-grained; z represents medium-grained; zc: medium-coarse grained; zx: medium-fine grained.

Table 5 Test and analysis data of the geological map spatial database of Beiliutumiao map-sheet, Inner Mongolia (K49E011021)

Data type	Data volume	Basic characteristics of data
Petrochemical analysis	176 pieces	11 major elements of volcanic and intrusive rocks
Trace element analysis	176 pieces	31 trace elements of volcanic and intrusive rocks
Isotopic age	10 pieces	LA-ICP-MS zircon U–Pb isotopic ages of volcanic, intrusive and clastic rocks

expression of various kinds of geological information is improved and standardized.

(3) Based on previous data and the results of the present project, we express the material composition and tectonic association of the Bainaimiao island-arc belt through field investigations of sedimentary formations and tectonic deformation sequence, and find that the Bainaimiao island-arc belt is characterized by Silurian adakite emplacement originating from the subducted plate, with intermediate-acidic volcano-sedimentary formation and near-EW tight folds and steep cleavages developed in the strata.

(4) We reclassify the sedimentary formation, igneous rock and tectonic deformation sequence of the Silurian, Permian, and Cretaceous eras in the Beiliutumiao map-sheet, and establish a relatively complete tectonic evolutionary series. We systematically construct the sedimentary formation and tectonic association of Paleozoic geobodies in the Bainaimiao area and their eras. Early Paleozoic island-arc intrusive rocks, previously classified as Ordovician, are re-classified as Silurian, with zircon U–Pb age ranging from 414.4 Ma to 434.2 Ma. The Paleozoic intrusive rocks are concentrated in Middle-Permian emplacement, displaying characteristics of continental margin arc granite.

Acknowledgments: The 1：50 000 Geological Map of Beiliutumiao Map-sheet, Inner Mongolia is the collective result of the hard work of all members of the project team. We were guided and supported by many mapping scientists in geological mapping and database construction, and would like to express our most sincere appreciation to all the experts and members of the field project team.

Notes:

❶ Regional Geological Survey Team of Geology and Mineral Resource Bureau of Inner Mongolia Autonomous Region. 1： 200 000 Regional Geological Survey Report of Xianghuang Banner Map-sheet, Inner Mongolia Autonomous Region. 1976.

❷ Geology and Mineral Exploration Institute of Inner Mongolia. Four 1：50 000 geological reports of Taigushengmiao and others in Xilingol League, Inner Mongolia Autonomous Region. 2008.

❸ Inner Mongolia Geological Exploration Institute of China Chemical Geology and Mine Bureau. Four 1：50 000 regional mineral and geological survey reports including Alashanmengfenghualiang, Inner Mongolia Autonomous Region. 2012.

❹ Geological Survey Institute of Inner Mongolia. Investigation Report on Mineral Prospects in Chaganhadamiao-Bieluwutu Area, Inner Mongolia. 2012.

References

Allen M B, Windley B F, Zhang C. 1993. Palaeozoic collisional tectonics and magmatism of the Chinese

Tien Shan, Central Asia[J]. Tectonophysics, 220(1–4): 89−115.

Allen M B, Engor A M C, Natalin B A. 1995. Junggar, Turfan and Alakol basins as Late Permian to Early Triassic extensional structures in a sinistral shear zone in the Altaid orogenic collage. Central Asia[J]. Journal of the Geological Society (London), 152(2): 32−338.

Bai J. 2003. Recovery of structural styles of orogenic belt and its tectonic environmental significance[J]. Geological Survey and Research, 26(1): 38−44, 51 (in Chinese with English abstract).

Coleman R G. 1989. Continental growth of Northwest China[J]. Tectonics, 8(3): 621−635.

Gao J, Li M S, Xiao X C, Tang Y Q, He G Q. 1998. Paleozoic tectonic evolution of the Tianshan orogen, northwestern China[J]. Tectonophysics, 287(1–4): 213−231.

Han B F, He G Q, Wang X C, Guo Z J. 2011. Late Carboniferous collision between the Tarim and Kazakhstan-Yili terranes in the western segment of the South Tian Shan Orogen, Central Asia, and implications for the Northern Xinjiang, western China[J]. Earth Science Reviews, 109: 74−93.

Jahn B M, Griffin W L, Windley B F. 2000. Continental growth in the Phanerozoic: Evidence from Central Asia[J]. Tectonophysics, 328(1): vii-x.

Jian P, Liu D Y, KrNer A, Windley B F, Shi Y, Zhang F Q, Shi G H, Miao L C, Zhang W, Zhang Q, Zhang L Q, Ren J S. 2008. Time scale of an early to mid-Paleozoic orogenic cycle of the longlived Central Asian Orogenic Belt, Inner Mongolia of China: implications for continental growth[J]. Lithos, 101(3–4): 233−259.

Li J J, Dang Z C, Zhao Z L, Shi Y R, Liu D Y, Li C, Qu W J, Wang C X, Fu C, Tang W L, Zhang T, Wang S G, Zhou H Y, Zhao L J, Liu X X. 2015. The Metallogenic Epochs of Bainaimiao Copper Deposit in Inner Mongolia[J]. Acta Geologica Sinica, 89(8): 1448−1457 (in Chinese with English abstract).

Li Y L, Zhou H, Brouwer F M, Xiao W, Wijbrans J R, Zhong Z. 2014. Early paleozoic to middle triassic bivergent accretion in the Central Asian Orogenic Belt: insights from zircon U-Pb dating of ductile shear zones in central Inner Mongolia, China[J]. Lithos, 205(9): 84−111.

Li Y J, Wang G H, Santosh M, Wang J F, Dong P P, Li H Y. 2018. Supra-subduction zone ophiolites from Inner Mongolia, North China: Implications for the tectonic history of the southeastern Central Asian Orogenic Belt[J]. Gondwana Research, 59: 126−143.

Li Y J, Wang G H, Santosh M, Wang J F, Dong P P, Li H Y. 2020. Subduction initiation of the SE Paleo-Asian Ocean: Evidence from a well preserved intra-oceanic forearc ophiolite fragment in central Inner Mongolia, North China[J]. Earth and Planetary Science Letters, 535: 116087.

Liu C F, Liu W C, Wang H P, Zhou Z G, Zhang H F, Tang Y J. 2014. Geochronology and Geochemistry of the Bainaimiao Metavolcanic Rocks in the Northern Margin of North China Craton[J]. Acta Geologica Sinica, 88(7): 1273−1287 (in Chinese with English abstract).

Liu M, Zhang D, Xiong G Q, Zhao H T, Di Y J, Wang Z, Zhou Z G. 2016. Zircon U–Pb age Hf isotope and geochemistry of Carboniferous intrusions from the Langshan area, Inner Mongolia: Petrogenesis and tectonic implications[J]. Journal of Asian Earth Sciences, 120: 139−158.

Liu Y, Teng F, Wang WL, Yang ZL. 2020. 1：50 000 Geological Map Database of Beiliutumiao Map-sheet, Inner Mongolia[DB/OL]. Geoscientific Data & Discovery Publishing System. (2020-06-30).

DOI: 10.35080/data.A.2020.P7.

Liu Y J, Li W M, Feng Z Q, Wen Q B, Franz Neubauer, Liang C Y. 2017. A review of the Paleozoic tectonics in the eastern part of Central Asian Orogenic Belt[J]. Gondwana Research, 43: 123−148.

Sengor A M C, Natalin B A, Burtman V S. 1993. Evolution of the Altaid tectonic collage and Palaeozoic crustal growth in the Eurasia[J]. Nature, 364: 299−304.

Qian X Y, Zhang Z C, Chen Y, Yu H F, Luo Z W, Yang J F. 2017. Geochronology and geochemistry of early paleozoic igneous rocks in Zhurihe Area, Inner Mongolia and their tectonic significance[J]. Earth Science, 42(9): 1472−1494 (in Chinese with English abstract).

Wang S Q, Hu X J, Zhao H L. 2019. New discovery of Late Carboniferous alkaline granite in the Honggeer area, Sonid Zuoqi, Inner Mongolia[J]. Geological Survey and Research, 42(2): 81−85 (in Chinese with English abstract).

Windley B F, Allen M B, Zhang C, Zhao Z Y, Wang G R. 1990. Paleozoic accretion and Cenozoic redeformation of the Chinese Tien Shan range, Central Asia[J]. Geology, 18(2): 128−131.

Windley B F, Alexeiev D, Xiao W J, Kröner A. 2007. Badarch G. Tectonics models for accretion of the Central Asian Orogenic Belt[J]. Journal of the Geological Society, 164: 31−47.

Wu F, Zhang S H, Zhao Y, Ye H. 2014. Emplacement depth and tectonic significance of Early Permian pluton in Inner Mongolia Guyang area, northern margin of North China block[J]. Geology in China, 41(3): 824−837 (in Chinese with English abstract).

Xiao W J, Windley B F, Hao J, Zhai M. 2003. Accretion Leading to Collision and the Permian Solonker Suture, Inner Mongolia, China: Termination of the Central Asian Orogenic Belt[J]. Tectonics, 22(6): 1069−1090.

Xiao W J, Windley B F, Badarch G, Sun S, Li J L, Qin K Z, Wang Z H. 2004. Palaeozoic accretionary and convergent tectonics of the southern Altaids: Implications for the growth of Central Asia[J]. Journal of the Geological Society, 161(3): 339−342.

Xiao W J, Mao Q G, Windley B F, Han C M, Qu J F, Zhang J E, Ao S J, Guo Q Q, Cleven N R, Lin S F, Shan Y H, Li J L. 2010. Paleozoic multiple accretionary and collisional processes of the Beishan orogenic collage[J]. American Journal of Science, 310: 1553−1594.

Xu B, Charvet J, Chen Y, Zhao P, Shi G Z. 2013. Middle Paleozoic convergent orogenic belts in western Inner Mongolia (China): framework, kinematics, geochronology and implications for tectonic evolution of the Central Asian Orogenic Belt[J]. Gondwana Research, 23(4): 1342−1364.

Xu B, Zhao P, Wang Y Y, Liao W, Luo Z W, Bao Q Z, Zhou Y H. 2015. The pre-Devonian Tectonic Framework of Xing'an–Mongolia Orogenic Belt (XMOB) in North China[J]. Journal of Asian Earth Sciences, 97(Part B): 183−196.

Xu Z, Han B F, Ren R, Zhou Y Z, Zhang L, Chen J F, Su L, Li X H, Liu D Y. 2012. Ultramafic-mafic mélange, island arc and post-collisional intrusions in the Mayile Mountain, West Junggar, China: implications for Paleozoic intraoceanic subduction-accretion process[J]. Lithos, 132–133: 141−161.

Yuan Y, Zong K Q, He Z Y, Klemd R, Jiang H Y, Zhang W, Liu Y S, Hu Z C, Zhang Z M. 2018. Geochemical evidence for Paleozoic crustal growth and tectonic conversion in the Northern Beishan Orogenic Belt, southern Central Asian Orogenic Belt[J]. Lithos, 302–303: 189−202.

Zhang W, Jian P. 2012. SHRIMP dating of the Permian Guyang diorite-granodiorite-tonalite suite in the northern margin of the North China Craton[J]. Geology in China, 39(6): 1593−1603 (in Chinese with English abstract).

Zhang W, Jian P, Kröner A, S hi, Y R. 2013. Magmatic and metamorphic development of an early to mid-Paleozoic continental margin arc in the southernmost Central Asian Orogenic Belt, Inner Mongolia, China[J]. Journal of Asian Earth Sciences, 72: 63−74.

Zhang X H, Gao Y L, Wang Z J, Liu H, Ma Y G. 2012. Carboniferous appinitic intrusions from the northern North China craton: geochemistry, petrogenesis and tectonic implications[J]. Journal of the Geological Society, 169: 337−351.

Zhao C, Su X L, Xue B, Cheng D J, Shi X J, Song T T, Zhang K. 2020. Zircon U-Pb dating and geochemical characteristics of granites in the area of Wula-Yingba, Kuchu, western Inner Mongolia[J/OL]. Geology in China, 1–22 [2020-07-07] (in Chinese with English abstract).

Zhao L, Niu B G, Xu Q Q, Yang Y Q. 2019. An analysis of Silurian- Carboniferous sedimentary and structural characteristics on both sides of Karamaili ophiolitic belt of Xinjiang and its significance[J]. Geology in China, 46(3): 615−628 (in Chinese with English abstract).

Zhao Y, Chen B, Zhang S H, Liu J M, Hu J M, Liu J, Pei J L. 2010. Pre-Yanshanian geological events in the northern margin of the North China Craton and its adjacent areas[J]. Geology in China, 37(4): 900−915 (in Chinese with English abstract).